Filler effects in resole adhesive formulations

Xuyang Wang

Thesis submitted to the faculty of the Virginia Polytechnic Institute and State University
in partial fulfillment of the requirements for the degree of

Master of Science

In

Macromolecular Science and Engineering

Charles E. Frazier, Chair

William Ducker

Young-Teck Kim

August 24, 2016

Blacksburg, Virginia

Keywords: organic filler, phenol formaldehyde, rheology, adhesive tack, wheat flour

Filler effects in resole adhesive formulations

Xuyang Wang

Abstract

This was a university/industry research cooperation with focus on how organic fillers affect the properties of phenol-formaldehyde resole (PF) resins that are formulated for veneer applications like plywood and laminated veneer lumber. The PF formulations studied in this work used fillers that were derived from walnut shell (*Juglans regia*), alder bark (*Alnus rubra*), almond shell (*Prunus dulcis*), and corn cob (furfural production) residue.

The chemical composition of all fillers was measured and compared to published data. The basic rheological behavior of the formulations was determined and used to develop an adhesive tack measurement based upon lubrication theory. In this work, the probe-tack test was adapted to a typical stress-controlled rheometer by using the normal force and displacement system to compress the adhesive between parallel plates. By employing a simple power law to describe the complex rheology of adhesives and a lubrication approximation for the viscous force, squeeze flow of adhesives between two flat, impermeable steels and between steel and porous wood can be successfully modeled. However, deviations from theory were encountered as related to the method of adhesive application. Both meniscus force in consequence of the surface tension of adhesive pull around the edge of plate and viscous force due to the viscosity of adhesive operate inside the meniscus when adhesive was spread on the entire surface by a hard roller. Such is probably the case when wood veneer is cold-pressed (pre-pressed) in plywood manufacture where viscosity and surface tension effects were both involved. Last but not least, rheological behavior and alkali modification of wheat flour was determined by rheological and infrared studies, respectively.

Acknowledgements

I would never have been able to achieve what I have without the guidance of all my committee members, help from friends, and support from my parents and girlfriend. I would like to take the time here to express my gratitude to them.

First and foremost, I would like to thank my advisor, Dr. Charles Frazier. Thanks to him for giving me a lot of inspiration on how to become a better scholar. He certainly is a great mentor for me and has been very generous in sharing his rich and valuable knowledge in the field I am involved. Before start working in his group, I chatted with several people who are close to him. One character that almost everyone mentioned is that he is demanding, but in a very reasonable way. After two years of time, I found this very true. He knows the perfect balance of challenging us and being there as support when we had difficulties and frustration. Through his depth of knowledge and enthusiasm, his respect for our different background and personal style, he made the past two years of mine very challenge and meaningful. Long story in short, I feel so very lucky to have met Dr. Frazier and have the opportunity to work with him.

I would also like to thank my other committee members, Dr. William Ducker and Dr. Kim-Teck Young; their support and expertise proved very beneficial to this work. In addition, I would like to thank the Wood-Based Composites Center (WBC) and Virginia Tech Graduate School for sponsoring this research. Special thanks to the people at William Valley Company who gave me great support for my study. Last but not least, I would like to thank all the wonderful people that helped me grow and to be success, especially David Jones, Rick Caudill, Linda Caudill, Debbie Garnand and so on. I am very grateful to my fellow colleagues in the wood adhesion group who made my two years of time so enjoyable and fulfilling, including Xing Yang, Guigui Wan, Mohammad Tasooji, Dr. Ann Norris, and Christa Stables.

Last, and most importantly, I would like to thank my mom and dad. There are not enough words to describe how thankful I am to both of them. Thanks for their endless amounts of love and support. I am forever indebted to them.

Table of Contents

List of Figures

List of Tables

Chapter 1 Literature review

In the manufacture of structural veneer-based wood composites, such as plywood and laminated veneer lumber, phenol-formaldehyde (PF) is the most commonly used base resin [1]. In veneer applications, PF adhesives are commonly formulated with lignocellulosic fillers, and proteinaceous extenders to reduce costs meet various performance criteria, including prepress tack, gap-filling properties, post-cure strength and durability, etc. [1,2] While the conventional PF/filler/extender formulations have been used for several decades, little work has been published on fundamental aspects of filler and extender effects on adhesive properties. Therefore, the effort described here is part of a university/industry research cooperation with a focus on how organic fillers and extender impact PF adhesive properties with special emphasis on adhesive tack measurement.

1.1 Phenol-formaldehyde resin

Phenol-formaldehyde, as the first synthetic polymer, is synthesized from the polycondensation of phenol with formaldehyde [3]. Typically, the formaldehyde is added to phenol in the chain-growth reaction that forms prepolymers at temperature less than 100 °C. Subsequently, a further cross-linking reaction occurs at temperature above 100 °C. Depending on the reagent ratios and pHs, two prepolymer types are produced. Novolaks are obtained with a deficiency of formaldehyde under acidic pH region, while resoles are formulated with an excess of formaldehyde under alkaline conditions [4-6]. Resoles have been extensively used as exterior-grade adhesives in the manufacture of structural veneer-based wood composites.

1.2 Fillers in phenol-formaldehyde adhesive

PF adhesives are commonly formulated with low-cost organic fillers. These fillers are typically derived from lignocellulosic biomass waste streams, such as nutshell, tree bark, and furfural-production residues. Fillers are generally considered to be inert and they serve to reduce resin costs and modify flow properties. They can also act as bulking agent, control adhesive rheological behavior and fill gaps and irregularities in the often cracked and irregular veneer surfaces. Addition of these fillers to liquid PF resins has been shown to reduce cost and improve properties of the veneer-based composites [7-10].

Three fillers, flours of walnut shell, red alder bark, and corn cob (furfural production) residue, were chemically characterized by Yang and Frazier [11]. The complete chemical constituents of the three fillers were adapted and summarized in Table 1-1 (Yang & Frazier, 2016). Alder bark and walnut shell was observed to contain the similar chemical compositions, where glucan and acid insoluble lignin corresponded to more than half of their chemical compositions. Their alkaline leachates also contained a similar chemical composition, where xylan and acid insoluble lignin dominated. While similar in composition, alder bark and walnut shell differed most in the quantity of extractives, xylan, and acid soluble lignin. However, the compositions of corn cob residue, where furfural is removed through a high-temperature pressure digester treatment followed by sulfuric acid hydrolysis, substantially differ from the other two fillers. Corn cob residue

contained a predominance of glucan and acid insoluble lignin but a small amount of xylan. In addition, it contained the extractives more than twice that found in the other fillers, released more lignin and much more glucan under alkaline leaching.

Table 1-1 Chemical constituents of alder bark (A), walnut shell (W), and corn cob residue (C) (% of total dry mass).

		Soxhlet extractives	Glucan	Xylan	Acid insoluble lignin	Acid soluble lignin
A		9.4				
W		4.5				
C		25.5				
Ex-free	A		26.4	16.8	31.3	1.4
	W		26.9	22.0	31.6	2.1
	C		46.7	0.9	27.2	0.4
Alkaline leachate	A		0.4	6.0	5.1	0.5
	W		1.5	8.9	6.0	0.5
	C		6.0	0.5	9.5	0.2

Source: Yang, X. and C. E. Frazier., Influence of organic fillers on rheological behavior in phenol-formaldehyde adhesives. International Journal of Adhesion and Adhesives (2016) 66: 93-98.

1.2.1 Nutshell flour

Nutshells, such as shells of walnuts, almonds, are lignocellulosic biomass obtained as agriculture residues. They were initially utilized in low-value agricultural applications, and were firstly introduced as fillers into plywood adhesives in 1942 [12]. The published chemical compositions of nutshells are summarized in Table 1-2 [13]. Walnut shells and almonds were found to be cellulose predominately in composition while pecans contained more lignin. Preston *el.al* [14] stated that, in general, 13C CPMAS NMR spectroscopy elucidated the overall organic composition of nutshells which were composed of cellulose, hemicellulose, and lignin, in proportions roughly similar to those found in hardwoods. Due to the unique chemical properties and availability of supply, walnut and almond shells have been utilized as fillers into plywood adhesives in the United States [12].

Table 1-2. Chemical constituents of different nutshells you have to cite the source of this table in the table or table title.

Nutshells	Ash (%)	Cellulose (%)	Hemicellulose(%)	Lignin (%)
Almond shell	2.6	36.9	17.9	24.8

Pecan shell	3.1	29.8	8.6	43.3
Black walnut shell	0.6	51.9	13.9	27.4
English walnut shell	1.0	54.2	11.9	16.8

Source: Toles C.A., Marshall W.E., Johns M.M., Phosphoric acid activation of nutshells for metals and organic remediation: process optimization, Journal of Chemical Technology and Biotechnology, 72 (1998) 255-63.

The finely divided almond (*Prunus dulcis)* shell products are derived from a large variety of almond shells that are by-products of almond shelling operations where the almond kernel is separated from the shell [13]. Finely grounded English walnut (*Juglans regia*) shell flour were firstly used as fillers into plywood adhesives in 1942 [12]. Walnut shells can resist fermentation and are stable in the wide range of temperature and pH conditions [14]. Pirayesh *et.al* [12] studied the addition of walnut/almond particle on the performance of urea-formaldehyde in particleboard. Significantly improved water resistance of the panels and greatly reduced formaldehyde emissions were observed with the addition of walnut/almond fillers. Therefore, the walnut/almond shells can be considered as an alternative filler in the manufacture of wood based composites.

1.2.2. Furfural digestion residue

In 1950, a by-product residue, results from a digester treatment and sulfuric acid hydrolysis in a variety of biomass materials, such as corncobs, rice hulls, was approved as an exterior adhesive filler [15]. These residues entered the filler market in 1951 as a conventional replacement for ground nutshells in PF adhesives. Among all available raw materials, corncobs approach the ideal furfural raw material due to its high pentosan yield and low ash content. Consequently, corn cob became the preferred raw material for furfural plants, and its resultant residue the preferred raw material as adhesive filler [16]. For the production of furfural, xylan, the major component of corn cob, is almost quantitatively hydrolyzed to xylose that was further dehydrated into furfural with about 50% yield [17]. The procedure was catalyzed by dilute sulfuric acid. Steam was introduced to bring the reactor to a selected temperature and then remove the produced furfural out of the reactor for recovery [18]. Xing and Frazier [19] reported that corn cob residue contained a predominance of 46.7% wt. glucan and 27.2% wt. acid insoluble lignin but less than 1% wt. of xylan. In addition, it contained 25.5% wt. of Soxhlet extractives and released more lignin and much more glucan under alkaline leaching than the other fillers.

2.2.3. Bark flour

Bark is the layer that is external to and surrounding the vascular cambium, and it accounts for about 10-15% wt. of the tree [20]. Bark can be roughly divided into inner bark or phloem, and dead outer bark or rhytidome. Through the grinding and classification operations employed on southern yellow-pin (*Pinus palustris*), Eberhardt and Reed [21] studied the strategy for improving the performance of plywood adhesive

mix fillers from pine bark. They found out that the filler rich in periderm tissue had superior performance over both the filler rich in obliterated phloem and that prepared directly from the bark as received. Douglas-fir (*Pseudotsuga menziesii*) bark as a filler entered the market in 1945 [22]. This bark that dispersed in boiling water and sodium hydroxide solution were ready to mix with resins, which enabled the improvement of workability of adhesive mix. However, alder bark (*Alnus rubra*) was by far the most widely used bark fillers in PF adhesives [20].

Bark is different from wood in chemical composition. In keeping with its heterogeneous structure, the chemical composition of bark exhibits great diversity. Harkin and Rowe [23] summarized the proximate composition of ash-free wood and bark, as shown in Table 1-3 (Harkin & Rowe, 1971), where bark generally contains more lignin and less polysaccharide.

Table 1-3 Proximate Composition of Ash-Free Wood and Barkcite table source here also

	Softwoods		Hardwoods	
	Wood	Bark	Wood	Bark
Lignin	25-30	40-55	18-25	40-50
Polysaccharides	66-72	30-48	74-80	32-45
Extractives	2-9	2-25	2-5	5-10
Ash	0.2-0.6	Up to 20	0.2-0.6	Up to 20

Source: Harkin J.M., Rowe J.W., Bark and its possible uses, USDA Forest Products Laboratory, Madison, WI, 1971.

1.3 Extenders in phenol-formaldehyde adhesive

Commercial wheat flour composes of protein, starch, non-starchy polysaccharides, and lipids. Protein constitutes 7-15% of common flour while starch makes up about 63-72% of flour on a 14% moisture basis [24]. Wheat flour are generally called “soft” or “weak” if gluten content is low, and are called "hard" or "strong" if they have high gluten content.

Gluten is the protein rich yellowish material, which is often referred as gluten complex [25]. Gluten includes two main protein groups that represents around 80% wt. of the total protein in commercial wheat flour. Soluble gliadins, which constitutes about 33% of total proteins, are monomeric globular proteins stabilized by intro-molecular disulphide bonds. Glutenins, on the other hand, are polymeric proteins connected by inter- and intro-molecular disulphide bonds [26].

The overall properties of treated wheat flour (i.e. hydration, alkali, heat) are determined by the functionality and behavior of its components. In terms of gluten, when hydrated,

gliadin provides viscous flow and extensibility [24]. Hydrated glutenin, however, is very elastic. Combined, these two properties yield a viscoelastic gluten complex [27, 28].

Starch, on the other hand, is a carbohydrate primarily comprised of two polysaccharides, namely amylose and amylopectin [29]. Van Hung et al. indicates that wheat starch contains approximately 25-28% amylose and 72-75% amylopectin [30]. Amylose and amylopectin are polymers of D-glucose. Amylose is a linear-type lightly branched molecule with α-1,4 glucosidic bonds while amylopectin has a branched structure formed by the addition of α-1,6 glucosidic bonds [26]. These polysaccharides exhibit excellent adsorption due to high hydrophilicity (hydroxyl groups), functional groups (primary amino, hydroxyl groups, acetamido), chemical reactivity and flexible polymer chain structure [24].

Starch functionality is based largely on its water absorbing ability which results in gelatinization and a loss of granular organization. In non-food applications, such as starch/flour-based adhesives, alkali gelatinization is of special interest. Maher [29] established that 3.5-3.8 meq/g of alkali is required for complete gelatinization. Ragheb [31] demonstrated physicochemical changes in the structure of treated starch by rheology and infrared studies. For example, they illustrated rheological behavior changed back and forth from non-Newtonian thixotropic to pseudoplastic as function of alkali concentration, ageing and temperature.

1.4 Adhesive tack

Tack is the property that controls the formation of a bond when an adhesive and a surface are brought into contact [1]. In practical terms, tack is the initial adhesive strength formed immediately upon contact, or immediately after consolidation pressure is applied. Preliminary to the final state of cure, tack may be considered as a “green” state of adhesion, and it will determine the requirements for moving a green bonded-assembly through a manufacturing process. With good tack, a green bonded-assembly can be moved rapidly without concern for delamination and associated manufacturing complications. Such is the case in plywood manufacture where a package of adhesive-coated wood veneer is cold-pressed (pre-pressed), and subsequently transferred into the hot-press for curing. Consequently, in plywood production adhesive tack is engineered to optimize the manufacturing process, and the wood/adhesive interaction that determines the final state of cure [2,3].

1.5 Rheology

Rheology is the science of deformation and flow of matter. Filled polymers are typically viscoelastic materials in the sense that their response to deformation lies in varying extent between that of viscous liquids and elastic solids [32].

Typically, additives such as extenders and fillers are added to change the characteristics of phenol-formaldehyde resin, which is used as primary binder in veneer-based structural wood composites. Xing and Frazier [11] showed that viscoelastic network structures

formed within the liquid formulations as a function of shear history, filler type, and filler particle size. The formation of viscoelastic structure could involve disintegration of filler particle aggregates on a non-colloidal scale, and/or colloidal effects within the liquid PF medium. In the latter case, colloidal structures could form among associated PF chains and also from proteins, polysaccharides, and lignins that leach from wheat flour and filler particles. The rheology of a particle suspension is a complex function of its physical properties and of processes that occur at the scale of the suspended particles. Colloid suspension is typically defined as a suspension of particles smaller than 10 microns [33]. Brownian forces, colloidal forces such as electrostatic forces and van der Waals forces, and hydrodynamic forces are the three basic types of forces that determine the rheological behavior of colloid suspensions [34].

Tirumkudulu et al. [35-37] studied the force measurements to pull apart two parallel surfaces separated by a thin film of Newtonian and non-Newtonian adhesives, respectively. The basic rheological behavior of adhesives was used to develop an adhesive tack measurement based upon lubrication theory.

1.6 Lubrication approximation

In 1886, Reynolds [38] published his analysis of hydrodynamic lubrication due to a thin macroscopic film of liquid confined between two moving solid surfaces. This theory is based on a simplification of the Navier-Stokes equations of continuum hydrodynamics by exploiting the special geometry of thin films [39].

Lubrication theory describes the flow of fluids (liquids or gases) in a geometry in which one dimension is significantly smaller than the others. From a historical perspective, the established theory (often referred to as the lubrication approximation) is applicable to both cases: the sliding of two surfaces past one another and the squeezing motion between two bodies [40, 41]. In this paper, the second case will be specifically emphasized.

Consider the squeezing motion in a thin film of liquid held between a circular disk and a parallel flat plate in the limit in which $h \ll R$, where h is the gap between plates, R is the radius of plates. A cylindrical coordinate system (r, θ, z) with its origin located on the plate along the axis of the disk was adopted. If the plate remains stationary, no-slip requires:

at $z = 0$, $\quad v_r = v_\theta = v_z = 0$

whereas the disk is moving:

at $z = h$: $\quad v_r = v_\theta = 0 \quad and \quad v_z = U = \frac{dh}{dt}$

Hydrodynamic force, F, required to squeeze a thin film of Newtonian fluid between two circular plates of radius, R, by moving the top plate at a constant speed of $|dh/dt|$ towards the bottom plate, is given by

$$F_Z = 2\pi \int_0^R rp(r,h)dr = \frac{3\pi\mu UR^4}{2h^3}$$

where h is the gap between plates, and μ is the viscosity of fluid. The force is kept positive in compression and negative in tension. The above relation is valid for very small gaps ($h/R << 1$) when the effects of both inertia and surface tension can be neglected.

Though it is more than 100 years since Reynolds lubrication theory was published, the utility of this theory still stands today. Cai and Bhushan [42] showed that meniscus and viscous forces occur during separation of two parallel plates in the normal direction for the measurement of tack. Viscous force occurs due to the viscosity of the liquid, was applied by lubrication theory. Tirumkudulu et al. [35-37] applied the lubrication equation to both Newtonian and non-Newtonian liquids between parallel plates and found very good agreement between predictions and experimental observation. Similarly, Derks et al. [43] have studied the cohesive failure of soft adhesives using lubrication approximation. Their predictions were tested against the experimental force-distance curves, and were found to provide an excellent description of the data for most cases. Francis et al. [44], on the other hand, studied fluid adhesion where a spherical probe and flat are bound by a high viscosity Newtonian polymer melt. They also found a useful correlation between the measured adhesive strength and work of separation through the application of lubrication approximation.

1.7 Reference:

[1] Pizzi A., Mittal K.L., Handbook of adhesive technology, revised and expanded, CRC Press, Boca Raton, FL, 2003.

[2] Selbo M.L., Adhesive bonding of wood, USDA Forest Service, Washington, D.C., 1975.

[3] Knop A., Scheib W., Chemistry and application of phenolic resins, Springer-Verlag, Berlin, Germany, 1979.

[4] Sellers T., Plywood and adhesive technology, M. Dekker, New York, 1985.

[5] Baekeland L., The synthesis, constitution, and uses of bakelite, Industrial & Engineering Chemistry, 1 (1909) 149-61.

[6] Pilato L., Phenolic resins: a century of progress, Springer-Verlag, Berlin, Germany, 2010.

[7] Pizzi A., Mittal K.L., Handbook of adhesive technology, M. Dekker, New York, 2003.

[8] Robertson J.E., Robertson R., Review of filler and extender quality evaluation, Forest

Prod J, 27 (1977) 30-8.

[9] Sellers T., A plywood review and its chemical implications, in: Goldstein I.S. (Ed.), Wood technology: chemical aspects, American Chemical Society, Washington, DC, 1977, pp. 270-82.44

[10] Waage S., Gardner D., Elder T., The effects of fillers and extenders on the cure properties of phenol-formaldehyde resin as determined by the application of thermal techniques, J Appl Polym Sci, 42 (1991) 273-8.

[11] Yang, X. and C. E. Frazier., Influence of organic fillers on rheological behavior in phenol-formaldehyde adhesives. International Journal of Adhesion and Adhesives (2016) 66: 93-98.

[12] Hamidreza Pirayesh , Hossein Khanjanzadeh Ayoub Salari., Effect of using walnut/almond shells on the physical, mechanical properties and formaldehyde emission of particleboard. Composites: Part B 45 (2013) 858–863

[13] Toles C.A., Marshall W.E., Johns M.M., Phosphoric acid activation of nutshells for metals and organic remediation: process optimization, Journal of Chemical Technology and Biotechnology, 72 (1998) 255-63.

[14] Preston C.M., Sayer B.G., What's in a nutshell: an investigation of structure by carbon-13 cross-polarization magic-angle spinning nuclear magnetic resonance spectroscopy, Journal of Agricultural and Food Chemistry, 40 (1992) 206-10.

[15] Brownlee H.J., Miner C.S., Industrial development of furfural, Industrial & Engineering Chemistry, 40 (1948) 201-4.

[16] Riera F.A., Alvarez R., Coca J., Production of furfural by acid hydrolysis of corncobs, Journal of Chemical Technology and Biotechnology, 50 (1991) 149-55.

[17] Binder J.B., Blank J.J., Cefali A.V., Raines R.T., Synthesis of furfural from xylose and xylan, ChemSusChem, 3 (2010) 1268-72.

[18] Bu L., Xing Y., Yu H., Gao Y., Jiang J., Comparative study of sulfite pretreatments for robust enzymatic saccharification of corn cob residue, Biotechnol Biofuels, 5 (2012) 87.

[19] Yang, X. and C. E. Frazier., Influence of organic fillers on surface tension of phenol-formaldehyde adhesives. International Journal of Adhesion and Adhesives (2016) 66: 160-166.

[20] Laks P.E., Hon D., Shiraishi N., Chemistry of bark, Wood and Cellulosic Chemistry, 7 (1991) 257-330.

[21] Eberhardt T.L., Reed K.G., Strategies for improving the performance of plywood adhesive mix fillers from southern yellow pine bark, Forest Prod J, 56 (2006) 64-8.

[22] Buamscha M.G., Altland J.E., Sullivan D.M., Horneck D.A., Cassidy J., Chemical and physical properties of douglas fir bark relevant to the production of container plants, HortScience, 42 (2007) 1281-6.

[23] Harkin J.M., Rowe J.W., Bark and its possible uses, USDA Forest Products Laboratory, Madison, WI, 1971.

[24] Atwell, W.A., Wheat flour, Eagan Press, 2001

[25] Weegels, P.L., Hamer, R.J., Schofield, J.D., Functional properties of wheat glutenin. Journal of Cereal Science 23 (1996) 1–18.

[26] Pidgeon, E. F., The application of crossflow membrane filtration to remediate wheat starch processing wastewater for reuse. Ph.D. dissertation, Griffith University, Chapter 1 (2006) 10-48.

[27] Uthayakumaran, S., Gras, P.W., Stoddard, F.L., Bekes, F., Effect of varying protein content and glutenin-to-gliadin ratio on the functional properties of wheat dough. Cereal Chemistry 76 (1999) 389–394.

[28] Borght, A.V.D., Goesaert, H., Veraverbeke, W.S., Delcour, J.A., Fractionation of wheat and wheat flour into starch and gluten: overview of the main processes and the factors involved. Journal of Cereal Science 41 (2005) 221-237

[29] Maher, G. G. : Alkali gelatinisation of flours. Starch/Starke 35 (1983), 271-276

[30] P. V. Hung, M. Yamamori, N. Morita., Formation of enzyme-resistant starch in bread as affected by high-amylose wheat flour substitutions. Cereal Chemistry. 82 (2005), 690-694

[31] Ragheb A.A., Tawfik S., Cairo D., Gelatinization of starch in aqueous alkaline solutions. Starch/Starke 46 (1995), 338-345

[32] Shenoy A.V., Rheology of filled polymer systems, Springer, Netherlands, 1999.

[33] Russel W.B., Saville D.A., Schowalter W.R., Colloidal dispersions, Cambridge university press, England, 1992.

[34] Van de Ven T., Colloidal hydrodynamics, Academic Press, Waltham, MA, 1988.

[35] M. Tirumkudulu, W. B. Russel, On the measurement of “tack” for adhesives." Physics of Fluids 15(6): 1588 (2003)

[36] M. Tirumkudulu, W. B. Russel, and T. J. Huang, “Measuring the ‘tack’ of waterborne adhesives,” J. Rheol. 47, 1399 (2003)

[37] Jha P.K., Tirumkudulu M.S., Measurement of tack of Newtonian liquids on porous substrates, Physics of Fluids 19, 123 (2007)

[38] Reynolds O., On the Theory of Lubrication and Its Application to Mr. Beauchamp Tower's Experiments, Including an Experimental Determination of the Viscosity of Olive Oil. *Proc. R. Soc. Lond.* 1886 **40**, 191-203, published 1 January 1886

[39] A. V. Nguyen., Historical Note on the Stefan–Reynolds Equations. Journal of Colloid and Interface Science 231, 195 (2000)

[40] S.J. Lee, M.M. Denn, M.J. Crochet, A.B. Metzner., Compressive flow between parallel disks: I. Newtonian fluid with a transverse gradient. Journal of Non -Newtonian Fluid Mechanics, 10 (1982) 3-30

[41] S.J. Lee, M.M. Denn, M.J. Crochet, A.B. Metzner., G.J. Riggins., Compressive flow between parallel disks: II. Oscillatory behavior of viscoelastic materials under a constant load. Journal of Non -Newtonian Fluid Mechanics, 14 (1984) 30 l-325

[42] Cai S., Bhushan B., Meniscus and viscous forces during separation of hydrophilic and hydrophobic surfaces with liquid-mediated contacts, Materials Science and Engineering R 61, 78 (2008)

[43] Derks D., Lindner A., Creton C., Bonn D., Cohesive failure of thin layers of soft model adheisves under tension, Journal of Applied Physics 93, 1557 (2003)

[44] Francis, B. A. and Horn, R. G. 2001, Apparatus-specific analysis of fluid adhesion measurements, Journal of applied physics, vol. 89, no. 7, pp. 4167-4174.

Chapter 2 Adhesive characterization

2.1 Introduction

In the manufacture of structural veneer-based wood composites, such as plywood and laminated veneer lumber, phenol-formaldehyde (PF) resoles are typically formulated with lignocellulosic biomass wastes as filler, proteinaceous and amylaceous materials as extender and other additives to meet various performance criteria, including prepress tack, gap-filling properties, post-cure strength and durability, etc. [1,2] Among the widely used PF/filler/extender formulations, fillers are generally considered to be inert, and they serve to reduce resin costs and modify flow properties [3]. They are typically organic flours derived from lignocellulosic biomass waste streams such as walnut (*Juglans regia*) and almond (*Prunus dulcis*) nutshell, red alder (*Alnus rubra*) bark, and furfural production residues, i.e. corn cob residue. On the other hand, extenders are amylaceous materials with some protein content that possess adhesive action and impact the rheological properties of adhesive. The conventional adhesive extender used is wheat flour [4]. While the conventional PF/filler/extender formulations have been used in the manufacture of structural veneer-based wood composites for several decades, the filler chemistry and viscoelastic network structure within these fluids have been the subject of little detailed analysis. Therefore, the present work, as a part of university/industry research cooperation, is aimed at investigating chemical constituents of fillers (walnut shell, almond shell, alder bark, and corn cob residue) and rheological properties within each formulation.

2.2 Experimental

2.2.1 Materials

2.2.1.1 Fillers and extender

Modal^{TM} alder bark (AB) filler, walnut shell (W) filler, almond shell (A) filler, corn cob residue (C) filler were kindly provided by Willamette Valley Company (Eugene, OR, USA). The alder species was *Alnus rubra*; the walnut tree species was *Juglans regia*, English walnut, representing an unknown mixture of tree varieties characteristic of commercial production in northern California, U.S.A. The almond species was *Prunus dulcis*; the subspecies of corn (*Zea mays*) was unknown. Wheat flour were hard wheat flours produced by Idaho Milling and Grain (IMG) in Malad, ID and provided by Willamette Valley Company (Eurene, OR, USA).

2.2.1.2 Other chemicals

Phenol-formaldehyde (PF) resin was a 14B346 resin, supplied by Arclin (pH = 8.0 - 12.5, solids content = 43 %). Sodium carbonate and 50 % sodium hydroxide used for adhesive formulation, were obtained from Willamette Valley Company (Eugene, OR, USA) and Fisher Scientific, respectively. 97% decalin (a mixture of isomers) used for density measurement was obtained from Pfaltz & Bauer (Waterbury, CT)

2.2.2 Compositional analysis

Compositional analysis was conducted on four unclassified fillers as received. The moisture content was determined according to ASTM D4442, where 10 g of air dry sample was heated at 103 ± 2 °C for 24 hr. [6]. The extractives content was determined according to NREL/TP-510-42619 using 190 proof ethanol extraction in a Soxhlet apparatus. [7]. Lignin and carbohydrate content in extractive-free samples were determined according to NREL/TP-510-42618 and NREL/LAP-004 [8, 9], respectively. Acid-soluble lignin was determined by UV-Visible spectrophotometry. Structural carbohydrates were analyzed by ion chromatography using sugar recovery standards (SRS). Ash content was determined by thermogravimetric analysis (TGA) using air dry samples that were heated to 1000°C at 20°C/min. Acid-insoluble lignin was determined by the difference between acid-insoluble residue from vacuum filtration and ash content. The mean chemical compositions reported here are based upon three measurements.

2.2.3 Adhesive formulation

Each filler type was formulated with PF resin with the addition of water, wheat flour, Na_2CO_3, and 50% NaOH as shown in Table 2-1 (Willamette Valley Company, Eugene, OR, USA). Compared to the low shear mixing procedure in Yang and Frazier's work [10], the current formulation (400 g) was prepared in a mixer (600 mL stainless steel container, IKA® high viscosity mixer with Cowles blade mixer) with step-wised increasing speed from 750 up to 1500 rpm.

Table 2-1 General PF adhesive formulation in mass fraction, applicable to all filler types.

Formulation contents	Weight %
Water	18.4
PF resin	22.8
(Mix 750 rpm, 30 sec)	
Filler	7.5
(Add at ~10 g/min)	
Extender (Wheat flour)	5.5
(Add at ~10 g/min)	
Sodium carbonate	0.5
(Add at ~10 g/min)	
Increase to 1200 rpm, mix 4 min	
Sodium hydroxide, 50%	3.0
(Add over ~1 min)	
Mix 1200 rpm, 10 min	
PF resin	42.3
Increase to 1500 rpm, mix 2 min	
Total mixture	100.0

2.2.4 Density measurement

Densities of fillers and wheat flour were measured at room temperature according to ASTM D854-10 [11] by using a 50 ml pycnometer with approximately 1 g dry sample dispersed in 97% decalin (a mixture of isomers). The density of PF resin was measured using a 10 mL volumetric cylinder where the cylinder was carefully filled in increments (n=10). Sample density was obtained from the linear slope of the mass/volume plot. The density value of sodium carbonate and 50% NaOH were obtained from their MSDS.

2.2.5 Rheological analysis

2.2.5.1 Steady-state flow

Rheological flow-curves were obtained for all adhesive formulations as a function of filler type, mass and volume fraction. The steady state two-step shear flow was employed with a concentric cylinder geometry (conical rotor:14 mm radius, 42 mm height; cup: 15 mm radius; gap: 1 mm; 25 °C) on TA instruments AR G2 rheometer. The flow-curves were obtained immediately after formulation mixing. The rheological analysis involved a two-step acquisition of sequential, steady-state flow curves as follows: Step 1) using no specimen pre-shear, steady- state flow analysis with increasing shear rate from 0.05 to 4000 /s and Step 2) steady-state flow analysis under decreasing shear rate from 4000 to 0.05 /s; the transition between steps 1 and 2 was immediate with no intervening equilibration time. The steady-state criterion was defined as less than 5% change in shear stress among three consecutive data points over a period not longer than 1 minute.

2.2.5.2 Creep and recovery

Formulations were subjected to more detailed analysis, where the same two-step flow was imposed, however three additional segments were added (named X, Y, and Z). Segment X occurred just prior to Step 1 (ramping-up); segments Y and Z respectively occurred immediately before and after Step 2 (ramping-down). Segments X, Y, and Z contained a 120 second creep/recovery followed by a frequency sweep; the applied stresses (0.05 Pa) were well within the linear response (determined separately using a 1 Hz stress sweep).

2.3 Results and discussion

2.3.1 Compositional analysis

The chemical constituents of fillers are shown in Table 2-2. Alder bark, almond and walnut shell contained similar chemical compositions, where glucan, xylan and acid insoluble lignin corresponded to a significant portion of the overall content. While similar in composition, they differed most in the quantity of extractives and xylan. Corn cob residue, however, substantially differed from the other three fillers, where extractives in corn cob residue were more than twice that found in other fillers. In addition, corn cob residue contains little xylan because it is removed during furfural production through a high-temperature pressure digester treatment followed by sulfuric acid hydrolysis [12]. The summative yields obtained ranged from good, as for corn cob residue, to poor as for almond shell. It might be expected that the compositions and summative yields for almond and walnut shell would be similar. Note however that almond shell had less

glucan than that reported in Toles *et al.*[13], so the low summative yield for almond shell might be related to an error in glucan determination; but no obvious problems were note during analysis. The chemical constituents of fillers are very comparable to that reported by Yang, Frazier [14], who studied the chemical composition of alder bark, walnut shell and corn cob residue, but not almond shell.

In terms of ash content, as shown in Table 3-4, corn cob residue and walnut shell has the highest and lowest ash content, respectively. This is higher than that reported by Sellers *et.al.* [15], but very similar to that reported by Yang and Frazier [16]. Moisture content of all air dry fillers, on the other hand, are shown in Table 2-3. Moisture content of 4-6% were observed in all fillers, where walnut shell and almond shell has the highest and lowest moisture content, respectively.

Table 2-2 Chemical composition (% of total dry mass) of alder bark (AB), walnut shell (W), almond shell (A), and corn cob residue (C), # measurements = 3. Values in parenthesis = standard deviation

	Extract.	**Acid insol. lignin**	**Acid sol. Lignin**	**Glu**	**Xyl**	**Ara**	**Gal**	**Man**	**ash**	**Total**
A	7.5 (0.2)	33.2 (2.4)	1.1 (0.1)	18.5 (1.1)	15.8 (1.9)	0.4 (0.1)	0.1 (0.0)	0.2 (0.0)	1.7 (0.2)	76.8
W	4.2 (0.3)	30.2 (1.9)	1.9 (0.0)	26.5 (0.8)	21.8 (1.3)	1.1 (0.1)	0.1 (0.0)	0.1 (0.0)	0.7 (0.1)	85.9
CCR	24.3 (0.7)	27.6 (1.8)	0.4 (0.0)	43.4 (2.1)	0.5 (0.1)	0.2 (0.0)	0.1 (0.0)	0.1 (0.0)	1.9 (0.2)	96.6
AB	9.6 (0.3)	31.3 (1.3)	1.5 (0.1)	25.8 (1.9)	17.2 (1.1)	0.7 (0.2)	0.6 (0.0)	0.4 (0.1)	2.2 (0.2)	87.1

Table 2-3 Moisture contents of organic fillers (% of total air-dried mass)

Filler	**% moisture (n=3)**
Almond shell	4.2 ± 0.1
Walnut shell	5.7 ± 0.1
Corn cob residue	4.5 ± 0.1
Alder bark	5.5 ± 0.1

2.3.2 Formulation rheology in mass and volume fraction

Densities of each component in the formulation are shown in Table 2-4. All filler and extenders' densities were measured by 97% decalin (mixture of isomers), a non-swelling agent, instead of water that was used by Yang and Frazier [14]. Table 2-4 also shows the comparison of filler densities measured by the two agents. The two sets of data are comparable, though density measured by water is expected to be slightly lower. Corn cob residue and almond shell having the highest and lowest densities were subsequently used to assess rheology in terms of mass and volume fraction.

Table 2-4 Measured densities (n=3) and reported* densities for components of adhesive formulations used in this work.

Component	Density (g/ml)	Density (g/ml) by Xing and Frazier [9]
Corn cob residue	1.65 ± 0.05	1.74 ± 0.06
Alder bark	1.59 ± 0.04	1.55 ± 0.03
Almond	1.35 ± 0.02	
Walnut	1.60 ± 0.03	1.60 ± 0.02
Wheat flour	1.39 ± 0.04	
Phenolic resin	1.18 ± 0.03	
50% NaOH*	1.52	
Sodium carbonate*	2.54	

The general formulation of PF adhesive in mass fraction (Column 1 in Table 2-5) was converted into volume fraction based on the density measurements in Table 2-4 (using corn cob residue as reference and basis of calculation). This derived volume fraction formulation (Column 2 in Table 2-5) was subsequently converted into mass fraction based on the densities of almond shell and other components in the formulation (Column 3 in Table 2-5), where the same volume fraction formulation was assumed between corn cob residue and almond shell as filler.

Table 2-5 PF adhesive formulation in mass and volume fractions

Formulation contents	Mass % (Applicable to all fillers)	Volume % (Derived from corn cob residue formulation)	Mass % (Almond shell as filler)
Water	18.4	21.6	18.6
PF resin	22.8	23.1	23.0
Filler	7.5	5.8	6.7
Extender (wheat flour)	5.5	4.6	5.5
Sodium carbonate	0.5	0.2	0.4
Sodium hydroxide, 50%	3.0	2.3	3.0
PF resin	42.3	42.8	42.8
Total mixture	100.0	100.0	100.0

Rheology analysis of adhesives was governed by accurate control of the volume fraction of fillers, wheat flour and other components in the formulation. A two-step rheological analysis was performed based on column 1 in terms of mass fraction and column 3, derived from volume fraction, listed in Table 3-5, where almond shell was used as filler. Figure 2-1 reveals that there was minor difference in the rheological behavior between the two formulations though mass fraction formulation had relatively higher filler content. Therefore, the original mass fraction formulation that is applicable to all filler types was still used for all future studies.

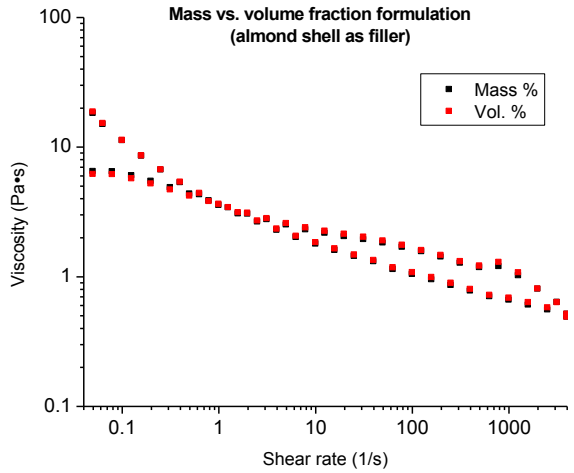

Figure 2-1. Comparison between mass and volume fraction formulations with almond shell as filler

2.3.3 Rheology of PF adhesives

Adhesive formulations in mass fraction as a function of filler type were subjected to the same two-step rheological analysis previously, where analysis began by ramping-up the shear rate from 0.05 to 4000 /s (Step 1), immediately followed by ramping-down the shear rate from 4000 to 0.05 /s (Step 2) with no intervening equilibration or delay.

Figure 2-2 shows the rheological behaviors of phenol formaldehyde (PF) resole resin, where a shear thinning behavior was observed. In contrast to the principally Newtonian PF base resin used by Yang and Frazier [10], the base resin in this work is clearly non-Newtonian. Non-Newtonian behavior in PF resoles is due to higher molecular weight and/or lower alkalinity [15]. Rheological behaviors of PF adhesives as a function of filler type were plotted in two graphs in Figure 2-3. Under increasing shear rate, all formulations exhibited a shear thinning behavior. As the shear rate was ramped-down (Step 2), all formulations regained viscosity. The presence or absence of structural reorganization [17,18] was indicated by whether a closed loop was formed at the low shear region. As shown in Figure 2-3, both alder bark and corn cob residue based formulations formed closed loops where the initial pre-shear structure appeared to reform. In contrast, almond and walnut shell based formulations exhibited cross-over

behavior in the low shear region, where adhesive was recovered to higher viscosity. This is suggestive of structural reorganization [17].

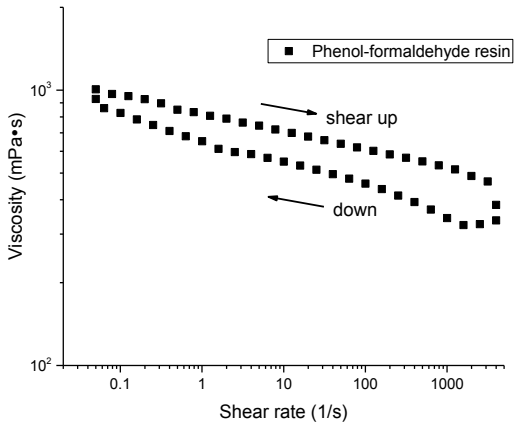

Figure 2-2. Rheological behavior of phenol formaldehyde (PF) resole resin

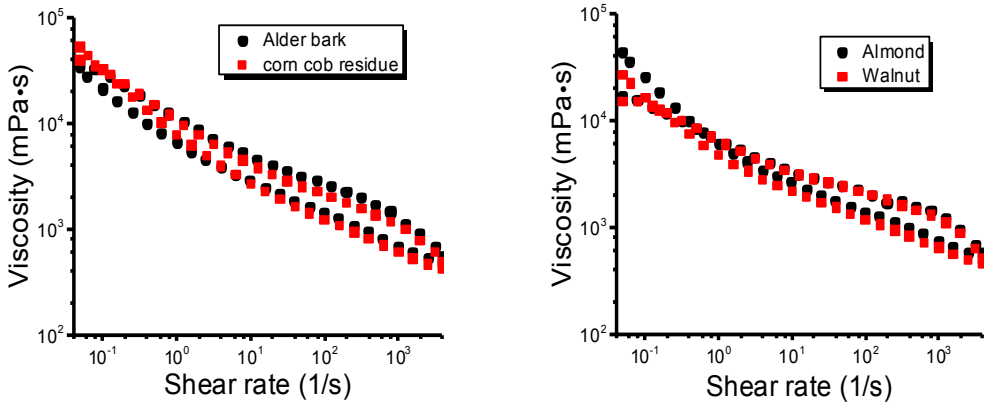

Figure 2-3. Rheological behaviors of PF with four fillers under a two-step acquisition

The rheological complexity of these PF/filler formulations is apparent under shear forces. The shear rate range in the present work includes those in the adhesive application such as pipe flow (10^0-10^3 s^{-1}), mixing and stirring (10^1-10^3 s^{-1}), spraying and brushing (10^3-10^4 s^{-1}) [16].

The flow behavior is very comparable to that reported by Yang and Frazier [10], who conducted the same rheological analysis as a function of filler type except for almond shell. According to their analysis, the complex rheological behavior within these formulations could arise from disintegration of filler particle aggregates on a non-colloidal scale, colloidal effects within the liquid PF medium and/or polymeric adsorption onto filler particle surfaces [17, 18]. Further studies on exact origin of these effects should be the subject of future research efforts.

2.3.4 Creep and recovery

The adhesive formulation (alder bark as filler) was subjected to more detailed analysis. In this case the same two-step flow was imposed, however three additional segments were added (named X, Y, and Z). Creep and recovery responses prior to Step 1 (ramping-up), before and after Step 2 (ramping-down) were plotted in Figure 2-4 respectively. Figure 2-4 indicates that creep response of the pre-shear character was nearly linear and principally viscous (segment X); Subsequent shearing during Step 1 flow caused increased elasticity (segment Y), which developed further as the viscosity recovered during Step 2 decreasing shear flow (segment Z). Creep and recovery response of adhesive apparently involved a transformation from mostly viscous to remarkably viscoelastic behavior.

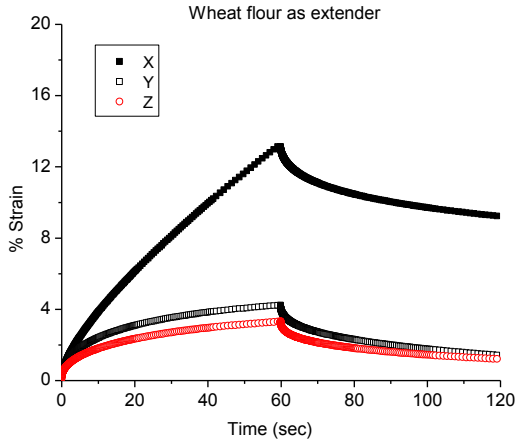

Figure 2-4. Creep/recovery responses, respectively X and Y, occurring before and after Step 1 ramping-up flow; Z occurred after Step 2 ramping-down flow. Alder bark as filler.

2.4 Summary

Fillers were chemically characterized with complete compositional analysis. Glucan, xylan and acid insoluble lignin corresponded to a significant portion of chemical compositions in alder bark, walnut and almond shell. Corn cob residue, however, substantially differ from the other three fillers, where extractives were more than twice that found in other filler, and little xylan content was observed. In term of moisture content and ash content, a 4-6% and 0.7-2.2 % wt. of dry mass were observed, respectively.

Two-step rheological analysis reveals that there was minor difference in the rheological behavior of mass and volume fraction formulations. Therefore, the mass fraction formulation was still used for future studies. Formulations as a function of filler type exhibited a complex flow behavior. Alder bark and corn cob residue based formulations formed closed loops where the initial pre-shear structure appeared to reform. In contrast, almond and walnut shell based formulations exhibited cross-over behavior in the low shear region, which is suggestive of structural reorganization. The creep and recovery

analysis revealed that adhesive apparently involved a transformation from mostly viscous to remarkably viscoelastic behavior. Many implications for impact of filler chemistry and rheological behavior on the flow properties of PF adhesives are feasible and should be the subject of future research efforts.

2.5 Reference

[1] Sellers T., Plywood and adhesive technology, M. Dekker, New York, 1985.

[2] Sellers T., A plywood review and its chemical implications, in: Goldstein I.S. (Ed.), Wood technology: chemical aspects, American Chemical Society, Washington, DC, 1977, pp. 270-82.

[3] Robertson J.E., Robertson R., Review of filler and extender quality evaluation, Forest Prod J, 27 (1977) 30-8.

[4] Sahoo S.C., Sill A., Pandey C.N., A Natural Additive Approaches to Enhance the Performance of Formaldehyde Based Adhesive for Plywood Manufacturing. International Journal of Innovative Science and Modern Engineering, 3(2014) 22-28.

[5] Yang, X. and C. E. Frazier (2016)., Influence of organic fillers on surface tension of phenol-formaldehyde adhesives. International Journal of Adhesion and Adhesives 66: 160-166

[6] ASTM D4442-15 Standard Test Methods for Direct Moisture Content Measurement of Wood and Wood-Based Materials, ASTM International, West Conshohocken, PA, 2015.

[7] Sluiter A., Hames B., Ruiz R., Scarlata C., Sluiter J., Determination of extractives in biomass. National Renewable Energy Laboratory, Golden, CO, 2008.

[8] Sluiter A., Hames B., Ruiz R., Scarlata C., Sluiter J., Templeton D., et al., Determination of structural carbohydrates and lignin in biomass, National Renewable Energy Laboratory, Golden, CO, 2008.

[9] Ehrman T., Determination of acid-soluble lignin in biomass, National Renewable Energy Laboratory, Golden, CO, 1996.

[10] Yang, X. and C. E. Frazier (2016). Influence of organic fillers on rheological behavior in phenol-formaldehyde adhesives. International Journal of Adhesion and Adhesives 66: 93-98.

[11] ASTM D854-14 Standard Test Methods for Specific Gravity of Soil Solids by Water Pycnometer, ASTM International, West Conshohocken, PA, 2014.

[12] Riera F.A., Alvarez R., Coca J., Production of furfural by acid hydrolysis of corncobs, Journal of Chemical Technology and Biotechnology, 50 (1991) 149-55.

[13] Toles C.A., Marshall W.E., Johns M.M., Phosphoric acid activation of nutshells for metals and organic remediation: process optimization, Journal of Chemical Technology and Biotechnology, 72 (1998) 255-63.

[14] Yang, X. and C. E. Frazier., Influence of organic fillers on surface tension of phenol-formaldehyde adhesives. International Journal of Adhesion and Adhesives (2016) 66: 160-166.

[15] Haupt R.A., Sellers T.J. Characterizations of phenol-formaldehyde resol resins, Ind Eng Chem Res 1994;33:693-7

[16] Yang, X., Organic fillers in phenol-formaldehyde wood adhesives. Ph.D. dissertation, Virginia Tech, Chapter 3 (2014) 61-70.

[17] Johansson K., Larsson A., Ström G., Stenius P., Adsorption of phenol-formaldehyde resin onto cellulose, Colloids and Surfaces, 25 (1987) 341-56.

[18] Stack K., Dunn L., Roberts N., Adsorption studies of phenolformaldehyde resin onto cellulose fibres, Colloids and Surfaces A: Physicochemical and Engineering Aspects, 70 (1993) 23-31

Chapter 3 Adhesive tack measurement

3.1 Introduction

Tack is the property that controls the formation of a bond when an adhesive and a surface are brought into contact [1]. In practical terms, tack is the initial adhesive strength formed immediately upon contact, or immediately after consolidation pressure is applied. Preliminary to the final state of cure, tack may be considered as a "green" state of adhesion, and it will determine the requirements for moving a green bonded-assembly through a manufacturing process. With good tack, a green bonded-assembly can be moved rapidly without concern for delamination and associated manufacturing complications. Such is the case in plywood manufacture where a package of adhesive-coated wood veneer is cold-pressed (pre-pressed), and subsequently transferred into the hot-press for curing. Wood veneer is typically not flat, but upon cold-pressing a flat panel results when tack is good. Furthermore, the cold-pressed panel remains flat, resists delamination, as is easily loaded into the hot-press. Otherwise, delamination prior to hot-pressing complicates material flow, and negatively impacts adhesive flow and cure properties due to excessive water evaporation. Consequently, in plywood production adhesive tack is engineered to optimize the manufacturing process, and the wood/adhesive interaction that determines the final state of cure [2,3].

The well-known probe-tack test measures the force needed to separate two surfaces bonded by a thin film of adhesive [4]. The probe, typically a flat circular plate, is closed upon adhesive that is deposited or coated onto a second flat plate. The probe is separated from the adhesive, and tack is recorded as the maximum tension force in absolute value or the work of separation [5]. Tirumkudulu et al. [6, 7] applied the Reynolds lubrication equation to Newtonian and non-Newtonian liquids between parallel-plates and found very good agreement between predictions and experimental observation. For simple Newtonian liquids, the compressive (closing) and tensile (opening) force is predicted as [8]:

$$F_Z = \frac{3\pi\mu R^4}{2h^3}\frac{dh}{dt} \qquad (1)$$

where h is the gap between plates, R is the circular plate radius, and μ is the liquid viscosity. Equation (1) is valid for very small gaps when the effects of surface tension can be neglected. Described here is the treatment of Tirumkudulu et al. [6, 7] applied to phenolic resole adhesives used to manufacture veneer-based wood composites like plywood and laminated veneer lumber. These adhesives are non-colloidal suspensions of organic fillers (like nutshell flours) and wheat flour extenders in an alkaline phenol-formaldehyde resole resin [2]. While the filler and extender particles are much larger than 1 micron, colloidal effects are suspected in these water-based systems due to the leaching of various biopolymers from filler and extender [9]. In this work, the probe-tack test was adapted to a typical stress-controlled rheometer by using the normal force and displacement system to compress the adhesive between parallel plates. We demonstrate that the treatment devised by Tirumkudulu et al. [8] provides a reasonably good

description of the tack test, but deviations from theory were encountered as related to the method of adhesive application.

3.2 Experimental

3.2.1 Materials

Modal^{TM} alder bark (AB), walnut shell (W), almond shell (A), and corn cob residue (C) fillers were kindly provided by Willamette Valley Company (Eugene, OR, USA). The walnut tree species was *Juglans regia*, English walnut, representing an unknown mixture of tree varieties characteristic of commercial production in northern California, U.S.A. The almond species was *Prunus dulcis*. The subspecies of corn (*Zea mays*) was unknown. Wheat flour extender (hard wheat) was produced by Idaho Milling and Grain (IMG) in Malad, ID and provided by Willamette Valley Company (Eurene, OR, USA). Phenol-formaldehyde (PF) resin was a 14B346 resin, supplied by Arclin (pH = 8.0 - 12.5, solids content = 43 %). Sodium carbonate (powder) and 50 % sodium hydroxide (liquid), used for adhesive formulation, were obtained from Willamette Valley Company (Eugene, OR, USA) and Fisher Scientific, respectively.

3.2.2 Wood specimen preparation

Wood specimens used were southern pine (*Pinus spp*.), smoothly cut using a planer, with dimensions of 50 × 50 × 5 mm (longitudinal x tangential x radial). They were kept at approximately 6% moisture content (equilibrated over saturated magnesium chloride solution).

3.2.3 Adhesive formulation

Each filler type was formulated with PF resin, water, wheat flour, Na_2CO_3, and 50% NaOH as shown in Table 3-1 (Willamette Valley Company, Eugene, OR, USA). Compared to the low shear rate mixing procedure in Yang and Frazier's work [9], the current formulation (400 g) was prepared in a mixer (600 mL stainless steel container, high shear mixer with a Cowles blade mixing head of 30 mm diameter) with step-wise increasing mixing rates of 750 up to 1500 rpm.

Table 3-1 PF adhesive formulation in mass fraction, applicable to all filler types.

Formulation contents	Weight %
Water	18.4
PF resin	22.8
(Mix 750 rpm, 30 sec)	
Filler	7.5
(Add at ~10 g/min)	
Extender (Wheat flour)	5.5
(Add at ~10 g/min)	
Sodium carbonate	0.5
(Add at ~10 g/min)	
Increase to 1200 rpm, mix 4 min	

Sodium hydroxide, 50%	3.0
(Add over ~1 min)	
Mix 1200 rpm, 10 min	
PF resin	42.3
Increase to 1500 rpm, mix 2 min	
Total mixture	100.0

Filler and wheat flour densities were measured at room temperature according to ASTM D854-10 [15] except that non-swelling 97% decalin (a mixture of isomers) replaced water as the solvent. The density of PF resin was determined from the linear slope of the mass/volume plot (10 mL volumetric cylinder carefully filled in 10 increments). The densities of sodium carbonate and 50% NaOH were obtained from their MSDS. All densities are listed in Table 3-2. Therefore, the volume fraction of fillers in the formulation ranges from 5.8 to 6.5 vol.%. Wheat flour, on the other hand, is about 4.6 vol.%.

Table 3-2 Measured densities (n=3) and reported* densities for components of adhesive formulations used in this work.

Component	Density (g/ml)
Corn cob residue	1.65 ± 0.05
Alder bark	1.59 ± 0.04
Almond	1.35 ± 0.02
Walnut	1.60 ± 0.03
Wheat flour	1.39 ± 0.04
Phenolic resin	1.18 ± 0.03
50% NaOH*	1.52
Sodium carbonate*	2.54

3.2.4 Tack measurement

Tack measurements were performed on a TA Instruments AR-G2 rheometer. Data acquisition was conducted with TA Instruments (standalone) data logger software with acquisition rate of 245 points per second. This utility runs in parallel with the rheometer's normal control software. Since there is no event synchronization, the data logger acquisition was started before the rheometer, with a lag of 1-2 seconds. A parallel plate geometry was employed with various sizes of top plates and a fixed 100mm diameter bottom plate, both made of stainless steel. After the adhesive was deposited on the bottom plate, experiments started in compression (closing step) with the top plate moving downward at a constant velocity until reaching a predetermined gap; thereafter the top plate moved upward (opening step), generating a tensile force. The normal force is detected by a transducer located beneath the bottom plate, and the calibration of this transducer was verified using standards of accurately known mass. Tack is indicated by both the maximum tensile force and energy (work) of detachment. Maximum tensile

force is defined as the maximum absolute value of force during the separation. Energy of detachment, on the other hand, is calculated by integration of area between the force-gap curve during the separation to the baseline where normal force equals to zero.

In order to mimic plywood manufacture, the tack test was adapted to wood surfaces of approximately 6% moisture content (equilibrated over saturated magnesium chloride solution). Wood specimens were southern pine (*Pinus spp*.) with dimensions of 50 × 50 × 5 mm (longitudinal x tangential x radial). Adhesive was applied to the tangential surface which was smoothly cut using a planer. The specimen was attached to the base by double-sided tape. Parallel plates with 40 mm diameter top plate and 100 mm diameter bottom plate was used. (Figure 3-1).

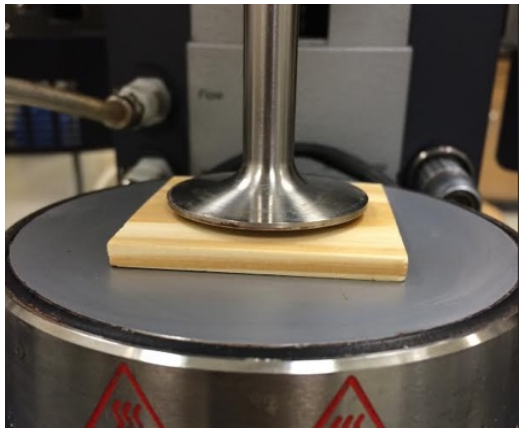

Figure 3-1: Tack test apparatus with wood as the bottom substrate

Adhesive was placed upon the tack measurement substrate using two methods, respectively referred to as the central drop and the roll coat methods. In the central drop method, sample was deposited on the center of the surface dropwise until the proper quantity (~0.25 mL) was achieved such that no squeeze-out would occur during the test. In the roll coat method, on the other hand, the adhesive was spread over the substrate using a hard roller.

When the adhesive was applied on the wood surface by the roll coat method, a predetermined mass of adhesives was spread on the entire surface. The specimen was subsequently attached to the bottom base by double sided tape. Experiment was conducted at 25°C with a 60 ± 2 s open time between sample deposition to start of experiment. 100 µm/s was used as probe velocity with 0 s dwell time between closing and opening steps.

3.2.5 Rheological analysis

Rheological flow-curves were obtained for adhesive formulations as a function of filler type. A steady state two-step shear flow was employed with a concentric cylinder geometry (conical rotor:14 mm radius, 42 mm height; cup: 15 mm radius; gap: 1 mm; 25 °C) on TA instruments AR G2 rheometer. The flow-curves were obtained immediately after formulation mixing. The rheological analysis involved a two-step

acquisition of sequential, steady-state flow curves as follows: Step 1) using no specimen pre-shear, steady-state flow analysis with increasing shear rate from 0.05 to 4000 s^{-1} and Step 2) steady-state flow analysis under decreasing shear rate from 4000 to 0.05 s^{-1}; the transition between steps 1 and 2 was immediate with no intervening equilibration time. The steady-state criterion was defined as less than 5% change in shear stress among three consecutive data points over a period not longer than 1 minute [9].

3.3 Results and discussion

3.3.1 Force-distance curve

Figure 3-2 is a plot of force and gap as a function of time. The gap curve demonstrates that the displacement rates remain linear, distinctly different from the nonlinear behavior Tirumkudulu [6,7] describes in the texture analyzer that employs a cantilever load cell. Therefore, the compliance of the instrument could be neglected in our study. The force curve exhibits the corresponding compression in the closing step, and tension upon opening where the tension was arbitrarily assigned a negative sign.

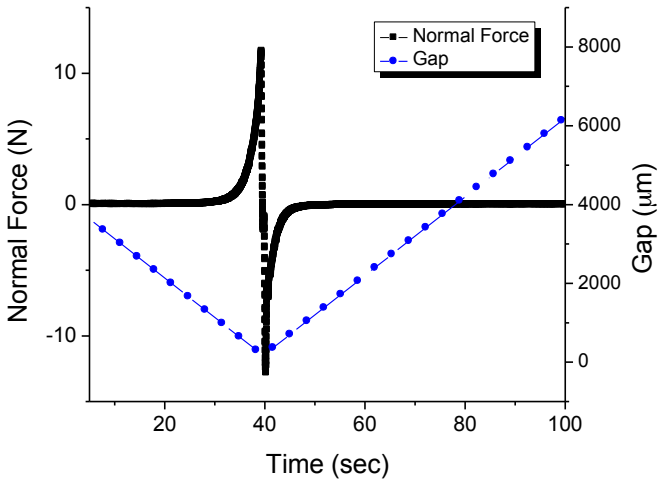

Fig. 3-2. Force/gap-time curve of formulated resole (alder bark as filler)

Figure 3-3 demonstrates the corresponding force-gap curve of formulated resole. The experiment was conducted at 25°C. 100 μm/s was used as probe velocity with 0 s dwell time between closing and opening steps. The end gap in the closing step was 200 μm. As labeled in Figure 3-3, the maximum tensile force and energy (work) of detachment are both used as tack indicator. Not easily seen in Figure 3-3 is that the actual minimum gap sometimes varies from the target (in this case 200 μm), typically on the order of 0μm to -6μm.

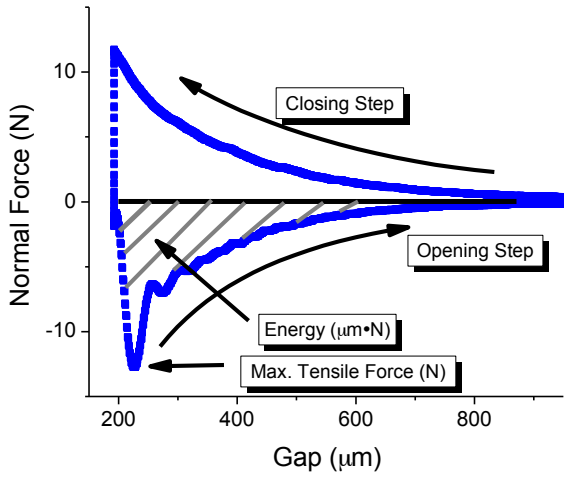

Fig. 3-3. Force-gap curve of formulated resole (alder bark as filler)

3.3.2 Application of lubrication approximation

The lubrication approximation (equation 1) is modified with the simple power law to describe the behavior of non-Newtonian fluids [7]. Hydrodynamic force, F, required to squeeze a thin film of shear-thinning liquid of viscosity $\mu = \mu_0\gamma^{n-1}$ (power-law equation) between two circular impermeable plates of radius, R, by moving the top plate at a constant speed of $|dh/dt|$ towards the bottom plate, is given by

$$F = \frac{2\pi\mu_0}{(n+3)} \times \left(\frac{2n+1}{n}\right)^n \times \frac{dh}{dt} \times \left|-\frac{dh}{dt}\right|^{(n-1)} \times \frac{R^{n+3}}{h^{2n+1}} \qquad (3)$$

where h is the gap between plates. μ_0 and n are input parameters in power law equation $\mu = \mu_0\gamma^{n-1}$, represent average viscosity of the fluid and deviation of fluid from Newtonian behavior respectively. μ, in the power law equation, is viscosity of the fluid at shear rate of γ:

$$\gamma_{avg} = \left|\frac{R}{h^2}\frac{dh}{dt}\right| \qquad (4)$$

Under constant probe velocity dh/dt and radius of plate R, equation (4) depicts the characteristic shear rate as a function of the gap h. Gap ranges from a predetermined initial position where the pull-off test starts to the distance of adhesive failure, which is estimated by visual observation. Therefore, based on Equation (4), in a test with gap ranges from 200 μm to ~3000 μm and probe velocity of 100 μm/s, the corresponding shear rate ranges from ~0.2 /s to 50 /s. In order to obtain the value of μ_0 and n in equation (3), power law equation $\mu = \mu_0\gamma^{n-1}$ was applied over the steady-state shear flow with shear range of 0.2 to 50 /s. In addition, the same rheology test over an arbitrary broad shear range from 0.05-4000 /s was also conducted for comparison purpose, as shown in

Figure 3-4.

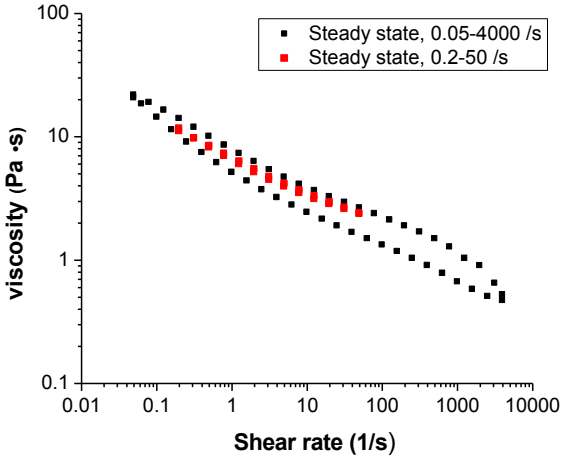

Figure 3-4. Comparison of viscosity plots between 0.05-4000 /s and 0.2-50 /s in a two-step acquisition of sequential steady-state shear flow

Figure 3-5 compares the experimental force-distance curve with the two predicted curves obtained by plugging the values of fixed experiment settings, μ_0 and n into equation (3). Corresponding data at the maximum tensile force was listed in Table 3.3. It was observed in Figure 3-5 that predictions of lubrication theory (Equation 3) captured well the main features of the force and gap profiles. As shown in Table 3.3, the curve with shear range characterized based on equation (4) results in a better prediction than the one with an arbitrary broad shear range.

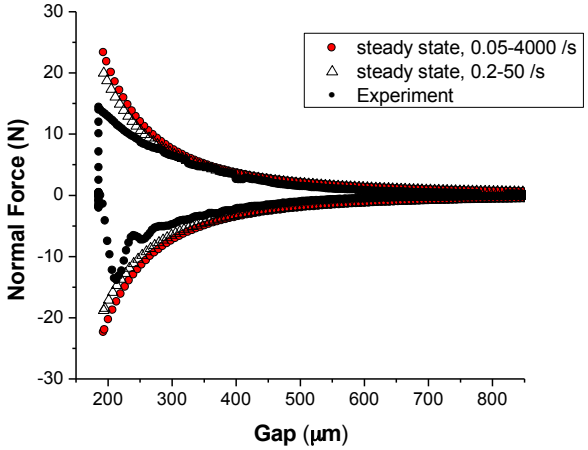

Figure 3-5. Comparison of experimental force-distance curve with predicted curves over two shear ranges. Sample was formulated with alder bark as filler. Experiments were conducted at 25°C with 200 μm end gap, 100 μm/s closing and opening rate, 0 second open time and dwell time.

Table 3.3 Comparison of maximum tensile force between experimental and predicted curves over two shear ranges. # measurements = 3 for experimental data, alder bark as filler.

	Normal force (-N)
Experiment	13.5 ± 0.2
Prediction (0.2-50 /s)	14.8
Prediction (0.05-4000 /s)	16.5

In addition, according to the lubrication equation (3), hydrodynamic force, F, should be dependent on several experiment settings, which are gap, radius of plates, and probe velocity. Therefore, a thorough study of effects of parameters on measured force was performed in the following section.

3.3.3 Effect of experimental parameters

Figure 3-6 and Figure 3-7 show that hydrodynamic force is dependent on radius of plates and gap. Its magnitude increases accordingly as radius of plate increases or gap decreases. In Figure 3-8, it shows that hydrodynamic force is dependent on probe velocity. It increases accordingly as opening and closing rate increases. Therefore, the previous hypothesis that hydrodynamic force, F, should be dependent on gap, radius of plates, and probe velocity was validated here.

The damped harmonic oscillation shape was observed during the separation where the force-distance curve oscillates with a constant frequency, validated from measurement of distance between valleys in the curve and with decreasing amplitude. This phenomenon was attributed to inertia effect, where initial high (yield) force was required to pull the sample. If the sample is purely elastic, due to the elastic component of the sample and/or instrument, the curve would keep oscillating at the same amplitude. However, the viscous damping force due to viscous component of the sample causes this oscillation to dampen.

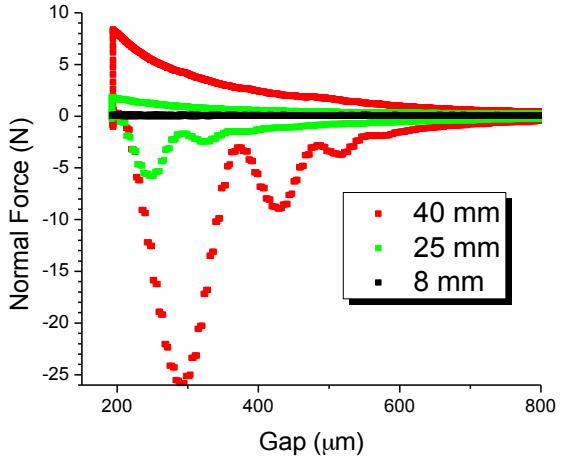

Figure 3-6. Effect of top plate diameter or contact area. Sample was formulated with alder bark as filler. Experiments were conducted at 25°C with 200 µm end gap, 100 µm/s closing and opening rate, 0 second open time and dwell time.

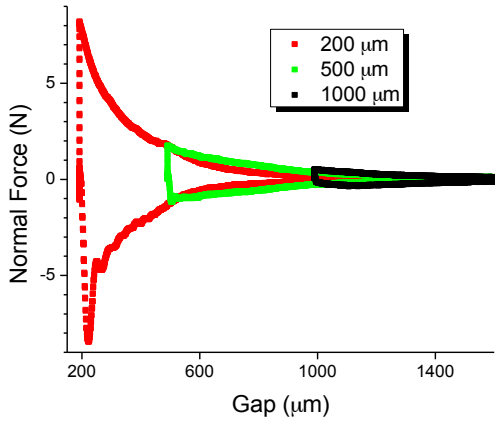

Figure 3-7. Effect of gap. Sample was formulated with alder bark as filler. Experiments were conducted at 25°C with 40 mm diameter top plate, 100 µm/s closing and opening rate, 0 second open time and dwell time.

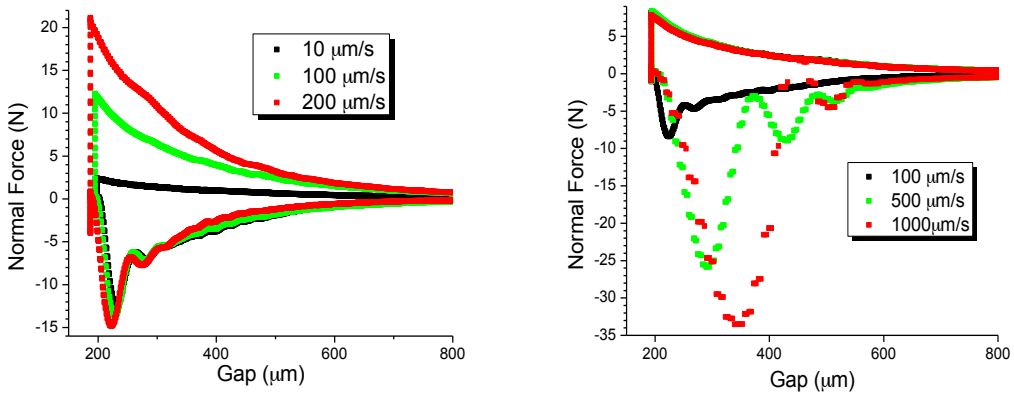

Figure 3-8. Effect of probe velocity in compression (left) and tension (right) steps. Sample was formulated with alder bark as filler. Experiments were conducted at 25°C with 40 mm diameter top plate, 200 µm end gap, 0 second open time and dwell time.

Moreover, possible correlation of adhesive tack among different formulations as a function of filler type is of special interest and could has great significance in terms of formulation modification. Therefore, formulations as a function of filler type were subject to the established tack test.

Figure 3-9 illustrates the effect of filler type on adhesive tack in terms of maximum tensile force and dissipating energy. It is clearly demonstrated that tack is filler-type dependent. Formulations increase tack compared to neat phenolic resin, with the alder bark based formulation having the highest tack.

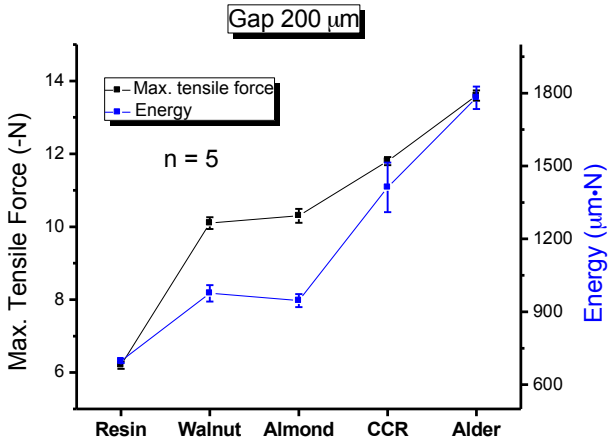

Figure 3-9. Effect of fillers. Experiments were conducted at 25°C with 40 mm diameter top plate, 200 µm end gap, 100 µm/s closing and opening rate, 0 second open time and dwell time.

3.3.4. Adaption to wood surface

Up to this point, tack of phenolic adhesives has been characterized by the modified probe-tack test conducted on flat, impermeable steel plates. However, in the plywood manufacture, adhesive is applied on the porous wood veneer instead. Therefore, we extended our study for squeeze flow of phenolic adhesive on porous wood as the bottom substrate where the flow in the gap is coupled to the fluid flow in the porous media.

Adhesives were formulated with the same procedure using alder bark as filler. Wood specimen was attached to the base with double-sided tape. Adhesive sample was applied on the center of wood surface dropwise. Experiments were conducted at 100 µm/s closing and opening rate with 40 mm diameter top plate, 200 µm end gap, 0 second dwell time and 60 ± 2 seconds open time.

Figure 3-11 compares the force-distance curves with steel on steel and steel on wood setup. Force-distance curves of steel on wood setup exhibited the same general behavior and distinguishable tack between formulations, but a smaller force compared to those of steel on steel. Table 3-3 shows the numerical difference of maximum force and energy on steel and wood and between formulations.

Tirumkudulu and Jha [14, 15] compared the squeeze flow of adhesives on impermeable steel and porous alumina substrates of different pore sizes/permeability. Small forces observed on porous substrates were attributed to the preferential flow of the liquid into the porous substrate than into the gap, where competition of spreading and penetration of liquid occurred. In addition, reduction in tack upon increase in pore size/permeability and initial penetration was also demonstrated in their study.

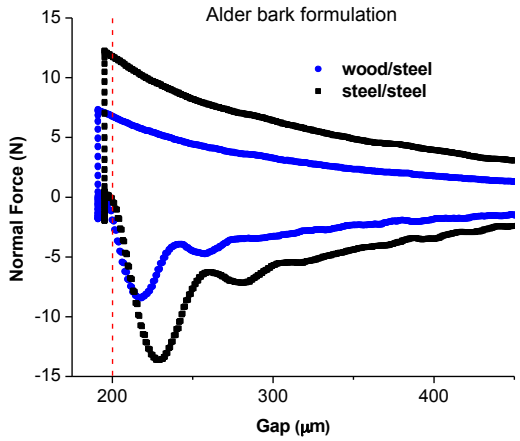

Figure 3-11. Comparison of force-distance curves between steel/steel and wood/steel by central drop method.

Table 3-3. Maximum tensile force and dissipating energy of the steel on steel and the steel on wood setup, # measurements = 3

	Steel/Steel		Wood/Steel	
Filler type	Max. tensile force (-N)	Energy (10^{-6} J)	Max. tensile force (-N)	Energy (10^{-6} J)
Almond shell	10.2 ± 0.0	946 ± 27	4.5 ± 0.1	692 ± 19
Alder bark	13.5 ± 0.2	1781 ± 46	7.6 ± 0.1	1116 ± 34

3.3.5. Force-distance curve by roll coat method

In all previous studies, adhesive was applied on the center of substrate dropwise, referred to as the central drop method. In this section, adhesive was spread on the entire surface by a hard roller, referred to as the roll coat method, which is closer to the case in plywood manufacture.

Figure 3-12 compares force-distance curves of alder bark based adhesive applied on wood surface by central drop and roller coat method, respectively. Surprisingly, an approximate 300 microns' degree of stretching till maximum tensile force and distinct shape of curve in the opening step were observed by roll coat method. The force-distance curves obtained by roll coat method deviates from the derived lubrication equation (equation 3). In addition, as shown in Table 3-4, though the maximum tensile forces are comparable by the two methods, energy of separation is significantly higher when adhesives were applied by roll coat method.

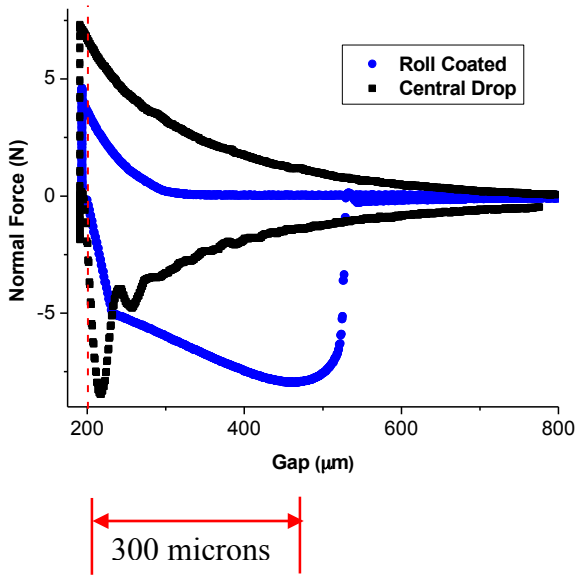

Figure 3-12. Comparison of force-distance curves between roll coat and central drop method on wood surface. Alder bark as filler.

Table 3-4. Maximum tensile force and dissipating energy by central drop and roll coat method on wood surface, alder bark as filler, # measurements = 3

Coat method	Max. tensile force (-N)	Energy (10^{-6} J)
Central drop	7.6 ± 0.1	1806 ± 36
Roll coat	7.7 ± 0.3	2038 ± 59

Furthermore, Figure 3-13 compares the force-gap curves by roll coat method on wood and steel substrates, respectively. Analogous to the force-gap curve on wood, the curve obtained when adhesive was applied on steel also deviates from lubrication equation, where an approximate 140 microns' plateau region followed by a sudden decay was observed. In addition, as shown in Table 3-5, the maximum force and energy are indeed lower when adhesive was applied on steel, which contradicts with the case observed by central drop method (Figure 3-11).

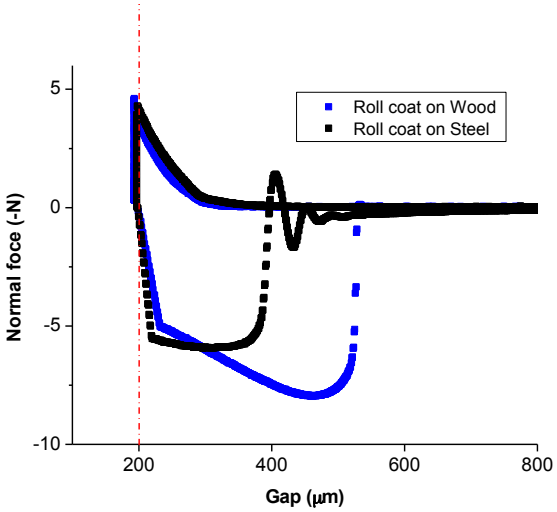

Figure 3-13. Comparison of force-distance curves when adhesive was applied by roll coat method on wood and steel, respectively. Alder bark as filler.

Table 3-5. Maximum tensile force and dissipating energy of roll coat method on steel and wood surfaces, alder bark as filler, # measurements = 3

Surface	Max. tensile force (-N)	Energy (10^{-6} J)
Steel	5.7 ± 0.2	783 ± 46
Wood	7.7 ± 0.3	2038 ± 59

3.3.6. Effect of surface tension

Cai and Bhushan [16] reviewed the studies of meniscus and viscous forces during separation of two parallel plates in the normal direction. Menisci was observed to form around the near-contacting and contacting asperities between two surfaces due to surface tension. The meniscus force can be obtained by integrating the Laplace pressure over the meniscus area and adding the surface tension effect acting on the circumference of the interface. Paddy *et. al* [17, 18] attributed the force exerted on the rod by the meniscus force in their rod-in-free-surface model. In contrast, Tirumkudulu et al. [6, 7], mentioned before, applied the lubrication equations (1,2) in the derivation of viscous force to their probe-tack experiments. Both of them found good agreement between predictions and experimental observation.

In terms of the modified probe-tack experiments in this Chapter, lubrication theory (equation 3) successfully modeled the squeeze flow of adhesives between two flat, impermeable steels and between steel and porous wood such that no squeeze-out would occur during the experiment. Surface tension was neglected where the viscous resistance of adhesives overwhelms the resistance to separation by surface tension. However, deviations from theory were encountered as related to the method of adhesive application. Meniscus force in consequence of the surface tension of adhesive pull around the edge of plate was observed to be significant when adhesive was spread on the entire surface by a hard roller. Therefore, both meniscus force and viscous force operate inside

the meniscus during the separation. Such is probably the case when wood veneer is cold-pressed (pre-pressed) in plywood manufacture where viscosity and surface tension effects were both involved.

3.3.7. Effect of open time

Study of open time was performed on experiments where adhesive was applied on wood substrate by roll coat method, where open time is defined as the time from when adhesive is applied to when experiment starts. Table 3-6 list the mean maximum force and energy as a function of filler type and open times. By comparing the data in the open time of 10 minute, alder bark based formulation was observed to have the highest tack. While the other three formulations seem to have indistinguishable value in terms of maximum force, but are clearly different in terms of energy. In terms of open time, on the other hand, a positive correlation was observed, where higher maximum force and energy were observed from longer open time.

Table 3-6. Mean maximum tensile force and dissipating energy of alder bark (AB), walnut shell (W), almond shell (A), and corn cob residue (C), # measurements = 3, open times are 1 min and 10 min

	Open time			
	1 min		10 min	
Filler type	Max. tensile force (N)	Energy (μm·N)	Max. tensile force (N)	Energy (μm·N)
Almond shell (A)	6.7 ± 0.2	1337 ± 43	6.9 ± 0.2	1422 ± 56
Walnut shell (W)			7.0 ± 0.3	1768 ± 67
Corn cob residue (CCR)			6.9 ± 0.2	1540 ± 62
Alder bark (AB)	7.7 ± 0.3	2038 ± 59	8.0 ± 0.1	2136 ± 78

3.4 Summary

The probe-tack test was adapted to a typical stress-controlled rheometer by using the normal force and displacement system to compress the adhesive between parallel plates. By employing a simple power law to describe the complex rheology of adhesives and a lubrication approximation for the viscous force, squeeze flow of adhesives between two flat, impermeable steels and between steel and porous wood can be successfully modeled, where viscous force, F, is dependent on gap, radius of plates, and probe velocity. Compare to steel, lower magnitude of force on wood was observed, where the flow in the gap is coupled to the fluid flow in the porous substrate. However, deviations from theory were encountered as related to the method of adhesive application. Meniscus force in consequence of the surface tension of adhesive pull around the edge of plate was observed to be significant when adhesive was spread on the entire surface by a hard roller. Therefore, both meniscus force and viscous force operate inside the meniscus where viscosity and surface tension effects were both involved. Last but not least, study of open time demonstrated that formulation with alder bark as filler exhibited the highest tack and a positive correlation between adhesive tack and open time.

3.5 **References**

[1] Creton C., Leibler L., How does tack depend on time of contact and contact pressure, Journal of Polymer Science: Part B: Polymer Physics, Vol. 34,545-554 (1996)

[2] Sellers T., Plywood and adhesive technology, M. Dekker, New York, 1985.

[3] Sellers T., A plywood review and its chemical implications, in: Goldstein I.S. (Ed.), Wood technology: chemical aspects, American Chemical Society, Washington, DC, 1977, pp. 270-82.

[4] ASTM D2979-01(2009) Standard Test Method for Pressure-Sensitive Tack of Adhesives Using an Inverted Probe Machine, ASTM International, West Conshohocken, PA, 2009

[5] Francis, B. A. and Horn, R. G. 2001, Apparatus-specific analysis of fluid adhesion measurements, Journal of applied physics, vol. 89, no. 7, pp. 4167-4174.

[6] M. Tirumkudulu, W. B. Russel, On the measurement of "tack" for adhesives." Physics of Fluids 15(6): 1588 (2003)

[7] M. Tirumkudulu, W. B. Russel, and T. J. Huang, "Measuring the 'tack' of waterborne adhesives," J. Rheol. 47, 1399 (2003)

[8] Reynolds O., On the Theory of Lubrication and Its Application to Mr. Beauchamp Tower's Experiments, Including an Experimental Determination of the Viscosity of Olive Oil. *Proc. R. Soc. Lond.* 1886 40, 191-203, published 1 January 1886

[9] Yang, X. and C. E. Frazier., Influence of organic fillers on rheological behavior in phenol-formaldehyde adhesives. International Journal of Adhesion and Adhesives (2016) 66: 93-98.

[10] Bird, R. B., R. C. Armstrong, and O. Hassager, Dynamics of Polymeric Liquids. Wiley, New York, 1977.

[11] Miranda J.A., Shear-induced effects in confined non-Newtonian fluids under tension, PHYSICAL REVIEW E 69, 016311 (2004)

[12] Poivet S., Nallet F., Gay C., Fabre P., Cavitation-induced force transition in confined viscous liquids under traction, Europhys. Lett. 62 (2), 244-250 (2003)

[13] Crosby A.J., Shull K.R., Creton C., Deformation and failure modes of adhesively bonded elastic layers, Journal of Applied Physics 88, 2956 (2000)

[14] Jha P.K., Measurement of tack of waterborne liquids on porous substrates, master thesis, Indian Institute of Technology (2006).

[15] Jha P.K., Tirumkudulu M.S., Measurement of tack of Newtonian liquids on porous substrates, Physics of Fluids 19, 123 (2007)

[16] Cai S., Bhushan B., Meniscus and viscous forces during separation of hydrophilic and hydrophobic surfaces with liquid-mediated contacts, Materials Science and Engineering R 61, 78 (2008)

[17] Padday, J. F., Pitt, A. R., and Pashley, R. M., Menisci at a Free Liquid Surface: Surface Tension from the Maximum Pull on a Rod J. Chem. Soc. Faraday Trans. 1 71, 1919 (1975).

[18] J. F. Padday, Menisci formed by a cone at a free liquid surface. An absolute method of surface tension measurement**,** J. Chem. Soc., Faraday Trans 1**,** 2827 (1979)

Chapter 4 Study of open time

4.1 Introduction

In Chapter 3, the well-known probe-tack test [1] was adapted by using controlled-stress rheometer for the measurement of pre-pressed tack of phenolic resole adhesives. Deviations from lubrication theory were encountered as related to the method of adhesive application. Therefore, the present work is aimed at investigating the experiments conducted on wood surface by roll coat method. Factorial design of experiment (DOE) was performed to investigate two factors, namely filler type and open time, on the response, indicated by maximum tensile force and energy of separation. Subsequently, statistical hypotheses tests, such as ANOVA and Student's t-test, were carried out to determine if any of these effects are statistically significant. [2,3]

4.2 Experimental

4.2.1 Fillers

Modal^{TM} alder bark (AB), walnut shell (W), almond shell (A), and corn cob residue (C) fillers were kindly provided by Willamette Valley Company (Eugene, OR, USA). The walnut tree species was *Juglans regia*, English walnut, representing an unknown mixture of tree varieties characteristic of commercial production in northern California, U.S.A. The almond species was *Prunus dulcis*. The subspecies of corn (*Zea mays*) was unknown.

4.2.2 Other chemicals

Wheat flour extender (hard wheat) was produced by Idaho Milling and Grain (IMG) in Malad, ID and provided by Willamette Valley Company (Eurene, OR, USA). Phenol-formaldehyde (PF) resin was a 14B346 resin, supplied by Arclin (pH = 8.0 - 12.5, solids content = 43 %). Sodium carbonate (powder) and 50 % sodium hydroxide (liquid), used for adhesive formulation, were obtained from Willamette Valley Company (Eugene, OR, USA) and Fisher Scientific, respectively.

4.2.3 Wood specimen

Wood specimens used were southern pine (*Pinus spp.*), smoothly cut using a planer, with dimensions of 50 × 50 × 5 mm (longitudinal x tangential x radial). They were kept at approximately 6% moisture content (equilibrated over saturated magnesium chloride solution).

4.2.4 Adhesive formulation

Each filler type was formulated with PF resin with the addition of water, wheat flour, Na_2CO_3, and 50% NaOH as shown in Table 4-1 (Willamette Valley Company, Eugene, OR, USA). Formulation (400 g) was prepared in a mixer (600 mL stainless steel container, IKA® high viscosity mixer with Cowles blade mixer head of 30 mm diameter) with step-wised increasing mixing rate of 750 up to 1500 rpm.

Table 4-1 PF adhesive formulation in mass fraction, applicable to all filler types.

Formulation contents	Weight %
Water	18.4
PF resin	22.8
(Mix 750 rpm, 30 sec)	
Filler	7.5
(Add at ~10 g/min)	
Extender (Wheat flour)	5.5
(Add at ~10 g/min)	
Sodium carbonate	0.5
(Add at ~10 g/min)	
Increase to 1200 rpm, mix 4 min	
Sodium hydroxide, 50%	3.0
(Add over ~1 min)	
Mix 1200 rpm, 10 min	
PF resin	42.3
Increase to 1500 rpm, mix 2 min	
Total mixture	100.0

4.2.5 Experiment procedure

A 4 x 3 factorial design of experiment (DOE) was performed with filler type and open time as two factors. Filler type has four levels: almond shell, walnut shell, alder bark and corn cob residue. Open time, defined as the time from when adhesive is applied to when experiment starts, has three levels: 10, 20 and 30 minutes. The response is indicated by maximum tensile force and energy of detachment.

All experiments were performed at specified test conditions. Adhesive was applied to the tangential wood surface that was attached to the instrument base by double-sided tape. Experiments were conducted at 25 °C, 100 μm/s closing and opening rate with 40 mm diameter top plate and 100 mm diameter base. 200 μm end gap and 0 second dwell time were used.

4.3 Results and discussions

4.3.1 Interpretation of raw data

Figure 4-1 illustrates the experimental force-distance curves as a function of filler type with open time of 10 minute as example. Raw data for 4 x 3 factorial design of experiment were plotted in Figure 4-2, where comparisons of the mean maximum force and energy as a function of filler type and open time were observed. Among fillers, alder bark based formulation was observed to have the highest tack. The other three fillers seem to have indistinguishable tack in terms of maximum force, but are clearly different in terms of energy. Therefore, energy of detachment is considered as a more sensitive tack indicator. In terms of open time, a positive correlation was observed, where higher maximum force and energy were observed from longer open time.

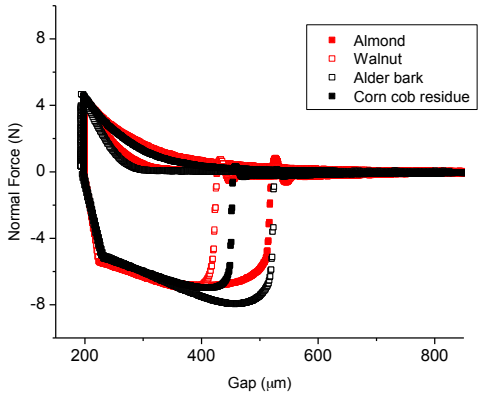

Figure 4-1. Force-distance curves of all formulations with open time of 10 minutes.

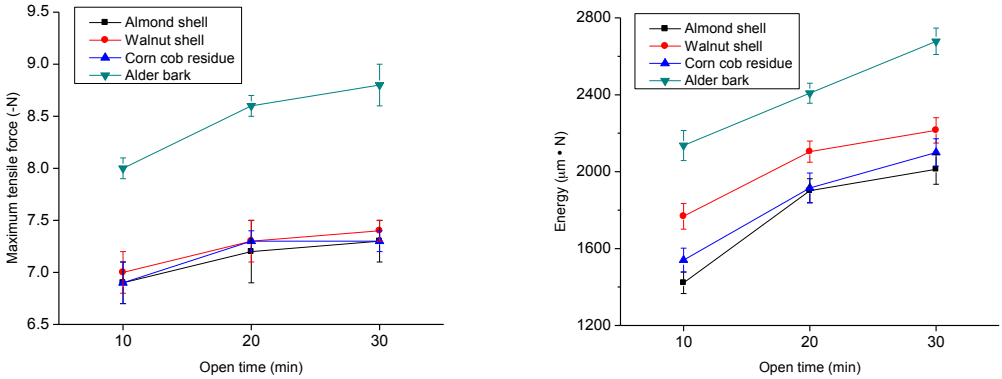

Figure 4-2. Comparison of maximum tensile force and dissipating energy among filler types and open times.

4.3.2. Statistical analysis

Effect plots help visualize the impact of each factor combination. However, statistical hypotheses tests are needed to determine if any of these effects are statistically significant [3,4].

4.3.2.1 An analysis of variance (ANOVA)

A single factor ANOVA test was conducted to test if there was a difference on measured tack as a function of filler type. Test conditions were summarized in Table 4-2.

Table 4-2: Test conditions

Factor:	Filler type

Level:	Almond shell, Walnut shell, Alder bark, Corn cob residue
Unit:	Maximum tensile force (N) / Energy (10^{-6} J)
Response variable:	Measured tack
Null hypothesis:	Formulations have the same mean tack
Alternative hypothesis:	Formulations have different mean tack

Table 4-3 shows the ANOVA test reports with filer type with two open times: 10 and 30 minutes. F-statistic (F stats.) is a ratio of variability between groups and within each level. P-value gives the likelihood of observing an F statistic at least this extreme, given that the null hypothesis is true. Thus, when the p-value is less than the significance level of 0.05, the effect size of that factor is statistically significant.

Table 4-3 shows that F crit. is smaller than F stat. and p-value is less than 5% significance level in terms of both maximum force and energy. Therefore, the null hypothesis, which states that the population means are all equal, is rejected to confirm that all levels of filler are significantly different.

Table 4-3. Single factor (filler type) ANOVA; open time: 10 and 30 minutes.

Output response	F stats. (10 min)	F stats. (30 min)	P-value	F crit.
Max. tensile force	25.83	76.11	0.00	4.07
Dissipating energy	93.07	158.64	0.00	4.07

4.3.2.2 Student's t-test

Student's t-test was used as a statistical method to identify if any two sets of data differ significantly. The two-sample *t*–test with one nominal variable, open time, and one measurement variable, either maximum force or energy, was conducted. The outcome is the acceptance or rejection of the null hypothesis (H_0), which states that the means of measured tack between two open times are the same. The differences observed (if any) are purely due to random errors. The alternative hypothesis (H_a) states exactly the opposite [7-9].

The t-value is a ratio of difference between groups and within groups**.** Every t-value has a p-value, which represents the probability of results from data sets happening by chance, given that the null hypothesis is true. A confidence level was predefined to be 95%, which states that in case of rejecting the null hypothesis (H_0), 5% or less certain of risk that the judgment was wrong.

Table 4-4 shows the numerical P-value calculated in Microsoft Excel. Comparison of P-value to value of 0.05 by 95% confidence level shows that besides the pair in corn cob residue based formulation in terms of maximum force, all other P-values are less than 5%. Thus, the null hypothesis must be rejected, indicating that the means of measured tack between the two open times are significantly different.

Table 4-4. Two-sample Student's t-test between data sets of two extreme open times (10 and 30 minutes) as a function of filler type

	P-value	
Pair	Max. tensile force	Dissipating energy
Walnut shell	0.02	0.00
Almond shell	0.04	0.00
Corn cob residue	0.07	0.00
Alder bark	0.00	0.00

4.4 Summary

4 × 3 Factorial design of experiment (DOE) was performed to investigate the effects of two factors: open time and filler type, on measured tack when adhesive was applied on wood surface by roll coat method. Alder bark based formulation was observed to have the highest tack. While, the other three fillers seem to have similar tack in terms of maximum force, but their response are clearly different in terms of energy. Therefore, energy of detachment is considered as a more sensitive tack indicator. In addition, positive correlation between tack and open time was observed in all filler types.

Single factor ANOVA test was performed to demonstrate that the means of measured tack as a function of filler type are statistically different. Two-sample Student's *t*–test, on the other hand, was used to demonstrate that the differences between measured tack in two open times are statically different except the case in corn cob residue based formulation.

4.5 References

[1] ASTM D2979-01(2009) Standard Test Method for Pressure-Sensitive Tack of Adhesives Using an Inverted Probe Machine, ASTM International, West Conshohocken, PA, 2009

[2] Kirk, R. E. 2003. Experimental Design. Handbook of Psychology. One:1:1–32

[3] Montgomery D.C., Experiments with a single factor. The Analysis of Variance. Design and Analysis of Experiments (third ed.), Wiley and Sons, New York (1991) pp. 50–94

[4] Winer B.J., Design and analysis of single factor experiments. Statistical Principles in Experimental Design (second ed.), McGraw Hill Book Company, New York (1971) pp 149–160

[5] Cuevas A., Febrero M., Fraiman R., An anova test for functional data. Vol 47 (11), 2004, pp. 11

[6] D.E. Hinkle, W. Wiersma, S.G. Jurs., One-way Analysis of Variance. Houghton Miffin Company, Boston (1982) pp. 251–279

[7] Hsu, P. L., Contribution to the theory of "Student's" t--test as applied to the problem of two samples. Statistical Research Memoirs, Vol 2, 1938, 1-24.

[8] J.C.F. de Winter., Using the Student’s t-test with extremely small sample sizes. Vol 18 (10), 2013

[9] L. Brown., The Conditional Level of Student's t-test. The Annals of Mathematical Statistics Vol. 38, No. 4 (Aug., 1967), pp. 1068-1071

Chapter 5 Wheat flour characterization

5.1 Introduction

In the manufacture of structural veneer-based wood composites, such as plywood and laminated veneer lumber, phenol-formaldehyde (PF) resoles are typically formulated with lignocellulosic fillers, and proteinaceous/amylaceous extenders to meet various performance criteria, including prepress tack, gap-filling properties, post-cure strength and durability, etc. [1,2] Among the widely used PF/filler/extender formulations, extenders have intrinsic adhesive action and also impact the adhesive rheological properties [3]. The conventional adhesive extender used is wheat flour, which is mainly composed of vital wheat gluten and wheat starch [4, 5]. Hydrated gluten is known to yield viscoelastic gluten complex [6-8]. Wheat starch is known to gelatinize under alkaline condition, which irreversibly disrupts the granular structure of starch. Gelatinized starch in alkali exhibits non-Newtonian thixotropic or pseudoplastic in various conditions [9-13]. Furthermore, Petrofsky [14] demonstrated the existence of starch-gluten interactions and dependence on wheat cultivars by changes in moduli in dynamic oscillation frequency sweep among isolated starch, vital gluten, and starch-gluten blends [15]. While the conventional PF/filler/extender formulations have been used in the manufacture of wood composites for several decades, effect of wheat flour as extender within these fluids have been the subject of little detailed analysis. Therefore, the present work, as a part of university/industry research cooperation, is aimed at investigating the effect of wheat flour on rheological properties of phenolic adhesives and alkali gelatinization phenomenon within adhesives.

5.2 Experimental

5.2.1 Materials

5.2.1.1 Fillers

Modal^{TM} alder bark (AB) filler, walnut shell (W) filler, almond shell (A) filler, corn cob residue (C) filler were kindly provided by Willamette Valley Company (Eugene, OR, USA). The alder species was *Alnus rubra*; the walnut tree species was *Juglans regia*, English walnut, representing an unknown mixture of tree varieties characteristic of commercial production in northern California, U.S.A. The almond species was *Prunus dulcis*; the subspecies of corn (*Zea mays*) was unknown.

5.2.1.2 Extender

Wheat flour were hard wheat flours produced by Idaho Milling and Grain (IMG) in Malad, ID and provided by Willamette Valley Company (Eurene, OR, USA). Vital wheat gluten and wheat starch were kindly provided by Archer Daniels Midland (Chicago, IL, USA).

5.2.1.3 Other chemicals

Phenol-formaldehyde (PF) resin was a 14B346 resin, supplied by Arclin (pH = 8.0 - 12.5, solids content = 43 %). Sodium carbonate and 50 % sodium hydroxide used for adhesive formulation, were obtained from Willamette Valley Company (Eugene, OR, USA) and Fisher Scientific, respectively.

5.2.2 Adhesive formulation

Each filler type was formulated with PF resin, water, wheat flour, Na_2CO_3, and 50% NaOH as shown in Table 5-1 (Willamette Valley Company, Eugene, OR, USA). Compared to the low shear rate mixing procedure in Yang and Frazier's work [16], the current formulation (400 g) was prepared in a mixer (600 mL stainless steel container, high shear mixer with a Cowles blade mixing head of 30 mm diameter) with step-wise increasing mixing rates of 750 up to 1500 rpm.

Table 5-1 PF adhesive formulation in mass fraction, applicable to all filler types.

Formulation contents	Weight %
Water	18.4
PF resin	22.8
(Mix 750 rpm, 30 sec)	
Filler	7.5
(Add at ~10 g/min)	
Extender (Wheat flour)	5.5
(Add at ~10 g/min)	
Sodium carbonate	0.5
(Add at ~10 g/min)	
Increase to 1200 rpm, mix 4 min	
Sodium hydroxide, 50%	3.0
(Add over ~1 min)	
Mix 1200 rpm, 10 min	
PF resin	42.3
Increase to 1500 rpm, mix 2 min	
Total mixture	100.0

5.2.3 Density measurement

Densities of fillers and wheat flour were measured at room temperature according to ASTM D854-10 [10] by using a 50 ml pycnometer with approximately 1 g dry sample dispersed in 97% decalin (a mixture of isomers). The density of PF resin was measured using a 10 mL volumetric cylinder where the cylinder was carefully filled in increments (n=10). Sample density was obtained from the linear slope of the mass/volume plot. The density value of sodium carbonate and 50% NaOH were obtained from their MSDS.

5.2.4 Rheological analysis

5.2.4.1 Steady-state flow

Rheological flow-curves were obtained for all adhesive formulations as a function of filler type, mass and volume fraction. The steady state two-step shear flow was employed with a concentric cylinder geometry (conical rotor:14 mm radius, 42 mm height; cup: 15 mm radius; gap: 1 mm; 25 °C) on TA instruments AR G2 rheometer. The flow-curves were obtained immediately after formulation mixing. The rheological analysis involved a two-step acquisition of sequential, steady-state flow curves as follows: Step 1) using no specimen pre-shear, steady- state flow analysis with increasing shear rate from 0.05 to 4000 /s and Step 2) steady-state flow analysis under decreasing shear rate from 4000 to 0.05 /s; the transition between steps 1 and 2 was immediate with no intervening equilibration time. The steady-state criterion was defined as less than 5% change in shear stress among three consecutive data points over a period not longer than 1 minute.

5.2.4.2 Creep and recovery

Formulations were subjected to more detailed analysis, where the same two-step flow was imposed, however three additional segments were added (named X, Y, and Z). Segment X occurred just prior to Step 1 (ramping-up); segments Y and Z respectively occurred immediately before and after Step 2 (ramping-down). Segments X, Y, and Z contained a 120 second creep/recovery followed by a frequency sweep; the applied stresses (0.05 Pa) were well within the linear response (determined separately using a 1 Hz stress sweep).

5.2.5 Sample preparation

Treatment of wheat starch and wheat flour with deionized water and alkali was performed as follows: 10 g of wheat starch or wheat flour were gradually added to 50 mL of deionized water and 50 mL 50% wt. NaOH solution separately over 1 minute. The mixture was gently stirred by glass rod. The mixture was mixed well, and settled at ambient temperature for 10 minutes.

5.2.6 Fourier transform infrared spectroscopy (FTIR)

Fourier transform Infrared spectroscopy (FTIR) was conducted on wheat starch and wheat flour that were treated with neutral deionized water, sodium hydroxide solution of 50% wt., and alkaline PF adhesive. All infrared spectra were obtained on a Thermo Scientific GladiATR^{TM} infrared spectrometer. All spectra were acquired with 64 scans and were processed using attenuated total reflection (ATR) and base-line correction.

5.3 Results and discussion

5.3.1 Rheology as a function of extender type

Commercial wheat flour composes of gluten, starch, non-starchy polysaccharides, and lipids, where gluten and starch account for nearly 80% wt. in wheat flour on a 14% moisture basis [4].

According to Idaho Milling and Grain (IMG), wheat flour used in this study composes of 13.7% wt. vital wheat gluten on a 11.1% wt. moisture basis. In order to study the effect of different components in wheat flour on adhesive rheology, phenolic adhesives were formulated with four different extenders: vital wheat gluten, wheat starch, starch/gluten blend, and whole wheat flour. Regarding starch/gluten blend, an 85/15 vol. ratio were used as an estimate to the actual wheat flour composition. All formulations as function of extender type were adjusted from mass fraction, shown in Table 6-1 previously, to volume fraction based on the density measurement shown in Table 5-2.

Table 5-2 Measured densities (n=3) and reported* densities for components of adhesive formulations used in this work.

Component	Density (g/ml)
Corn cob residue	1.65 ± 0.05
Alder bark	1.59 ± 0.04
Almond	1.35 ± 0.02
Walnut	1.60 ± 0.03
Wheat flour	1.39 ± 0.04
Vital wheat gluten	1.31 ± 0.03
Wheat starch	1.45 ± 0.04
Phenolic resin	1.18 ± 0.03
50% NaOH*	1.52
Sodium carbonate*	2.54

All formulations as a function of extender type were subjected to a two-steps steady-state flow. Figure 5-1 reveals that formulations with wheat flour, wheat starch and starch/gluten blend exhibited similar behaviors, whereas formulation with gluten as extender has a distinct behavior with much higher viscosity. Furthermore, Figure 6-2 compares the PF adhesives formulated with wheat flour and starch/gluten blend in shear stress-shear rate curve. It was observed that the rheological behavior of formulation with starch/gluten blend correlates exceptionally well with the conventional formulation with wheat flour. Therefore, starch/gluten blend appears to be a reasonable model for whole wheat flour.

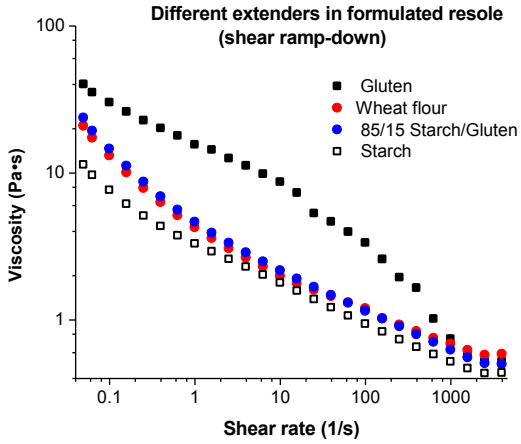

Figure 5-1. Rheological behaviors of PF with four extenders under a two-step acquisition (alder bark as filler)

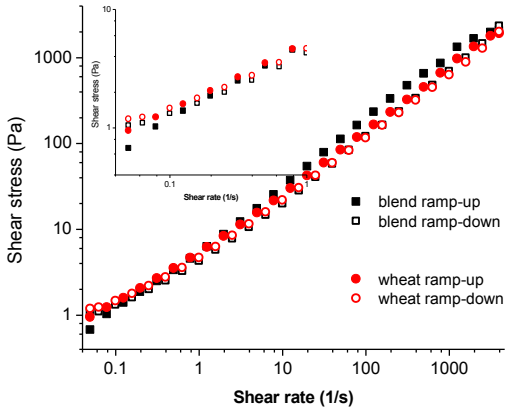

Figure 5-2. Rheological behaviors of PF with wheat flour and starch/gluten blend as extender under a two-step acquisition (alder bark as filler)

5.3.2 Creep and recovery

Formulations with wheat flour and starch/gluten as extender were subjected to more detailed analysis. In this case, the same two-step flow was imposed, however three additional segments were added (named X, Y, and Z). Creep and recovery responses prior to Step 1 (ramping-up), before and after Step 2 (ramping-down) were plotted in Figure 5-3 respectively. Figure 5-3 indicates that creep response of the pre-shear character of formulations with wheat flour and starch/gluten as extender was nearly linear and principally viscous (segment X); Subsequent shearing during Step 1 flow caused increased elasticity (segment Y), which developed further as the viscosity recovered during Step 2 decreasing shear flow (segment Z) in the formulation with wheat flour. Creep and recovery in both formulations apparently involved a transformation from mostly viscous to remarkably viscoelastic behavior.

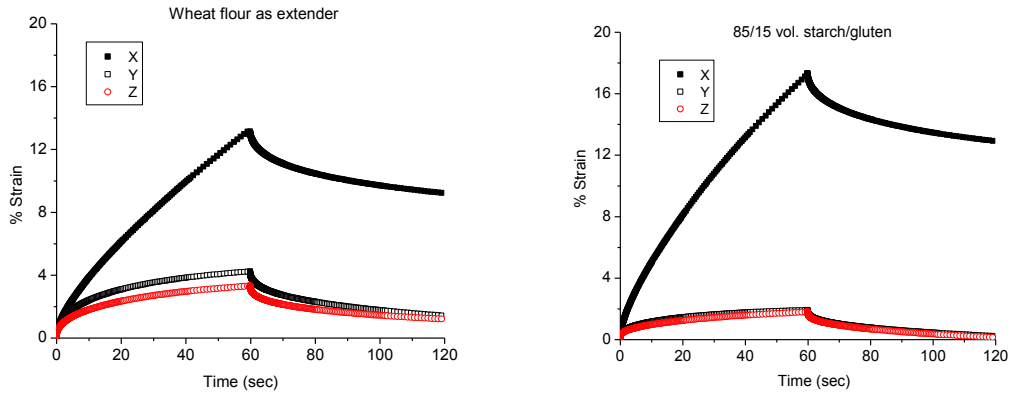

Figure 5-3. Creep/recovery responses, respectively X and Y, occurring before and after Step 1 ramping-up flow; Z occurred after Step 2 ramping-down flow.

5.3.3 Starch gelatinization

In the present study, infrared spectroscopy (IR) was conducted to investigate the behavior of wheat flour towards gelatinization under the action of sodium hydroxide solution and alkaline PF adhesive. Figure 5-4 compares the IR spectra of wheat starch and wheat flour that were treated with deionized-water and 50% NaOH solution at ambient temperature. The comparison indicates the appearance of the absorption band at 2800-2900 cm^{-1} of wheat starch and flour in alkali. In addition, infrared spectroscopy was conducted on neat phenolic resin and adhesive formulation with alder bark as filler. The appearance of the shoulder near ~2900 cm^{-1} in formulated adhesive was attributed to gelatinized flour, as shown in Figure 5-5.

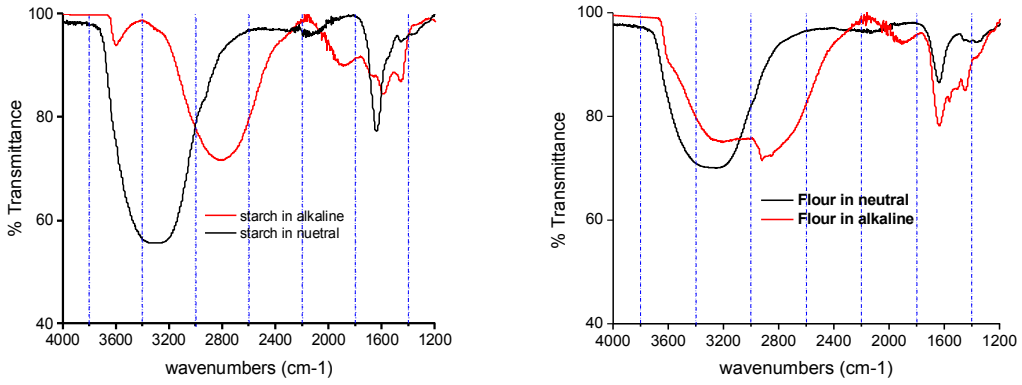

Figure 5-4. IR spectra of wheat starch and wheat flour in alkaline and neutral media

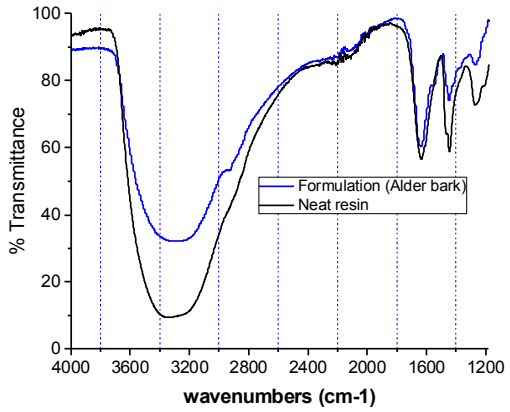

Figure 5-5. IR spectra of neat phenolic resin and formulation with alder bark as filler

Furthermore, the time required for flour gelatinization in formulated adhesive was studied. Fresh-made adhesive formulated with alder bark as filler were left at ambient temperature for 1 minute, 30 minute and 1 hour before testing. Figure 5-6 compares the IR spectra of adhesive that were tested at the three predetermined times. It was shown that gelatinization as function of time occurs in PF adhesive by the appearance of the shoulder near ~2900 cm^{-1} in Figure 5-6.

In conclusion, it is clear from the infrared spectra that alkali modification of wheat flour that composes of roughly 75% wt. starch is accompanied by some changes in the physico-chemical structure of starch. Gelatinization occurs in PF adhesive suggests that, the presence of alkali treatment increases the affinity of starch granules to water. As a consequence, swelling of starch granules occurs very fast and results in significant increment in granules size [11-13].

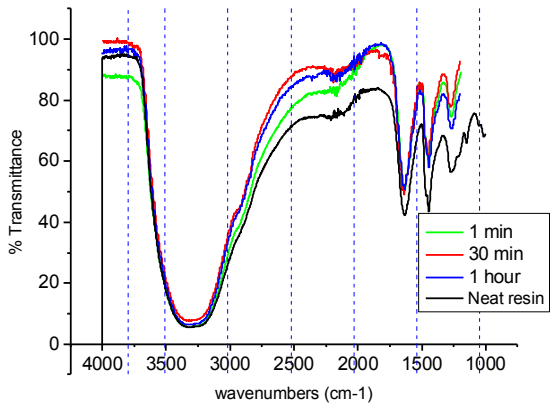

Figure 5-6. Time study of flour gelatinization in PF adhesive (alder bark as filler)

5.4 Summary

PF/wheat flour/organic filler formulations are well established technologies for the commercial manufacture of veneer-based wood composites, and yet much remains unknown about effect of wheat flour as extender within these fluids and the corresponding impact on adhesive rheology. It was shown that the 85/15 vol. starch/gluten blend appears to be a reasonable model for whole wheat flour. Creep and recovery response apparently involved a transformation from mostly viscous to remarkably viscoelastic behavior in formulations with wheat flour and starch/gluten. In addition, Infrared study showed that alkali modification of wheat flour is accompanied by some changes in the physico-chemical structure of starch. Gelatinization as a function of time was observed in PF adhesive. Investigation of filler/wheat flour interactions by using the starch/gluten model and infrared spectroscopy are feasible and should be the subject of future research efforts.

5.5 Reference:

[1] Sellers T., Plywood and adhesive technology, M. Dekker, New York, 1985.

[2] Sellers T., A plywood review and its chemical implications, in: Goldstein I.S. (Ed.), Wood technology: chemical aspects, American Chemical Society, Washington, DC, 1977, pp. 270-82.

[3] Robertson J.E., Robertson R., Review of filler and extender quality evaluation, Forest Prod J, 27 (1977) 30-8.

[4] Atwell, W.A., Wheat flour, Eagan Press, 2001

[5] Sahoo S.C., Sill A., Pandey C.N., A Natural Additive Approaches to Enhance the Performance of Formaldehyde Based Adhesive for Plywood Manufacturing. International Journal of Innovative Science and Modern Engineering, 3(2014) 22-28

[6] Weegels, P.L., Hamer, R.J., Schofield, J.D., Functional properties of wheat glutenin. Journal of Cereal Science 23 (1996) 1–18.

[7] Uthayakumaran, S., Gras, P.W., Stoddard, F.L., Bekes, F., Effect of varying protein content and glutenin-to-gliadin ratio on the functional properties of wheat dough. Cereal Chemistry 76 (1999) 389–394.

[8] Borght, A.V.D., Goesaert, H., Veraverbeke, W.S., Delcour, J.A., Fractionation of wheat and wheat flour into starch and gluten: overview of the main processes and the factors involved. Journal of Cereal Science 41 (2005) 221-237

[9] Alexander R.J., Krueger R.K., Plywood adhesives using amylaceous extenders comprising finely ground cereal-derived high fiber by-product, Washington, DC: U.S. Patent and Trademark Office, 1978.

[10] Maher, G. G. : Alkali gelatinisation of flours. Starch/Starke 35 (1983), 271-276

[11] Wootton, M., D. Weeden, and N. Munk: A rapid method for the estimation of starch gelatinisation in processed foods. Food Technol.in Aust., 23 (1971), 612-615.

[12] Wootton M., Ho P., Alkali gelatinization of wheat starch. Starch/Starke 41 (1989), 261-265.
[8] Muher, G. G.: Alakali gelatinisation of starches. Starch/Starke 35 (1983), 226-234

[13] Ragheb A.A., Tawfik S., Cairo D., Gelatinization of starch in aqueous alkaline solutions. Starch/Starke 46 (1995), 338-345

[14] Petrofsky K.E., Hoseney R.C., Rheological properties of dough made with starch and gluten from several cereal sources. Cereal Chem. 72(1995): 53-58.

[15] Kuktaite R., Larsson H., Johansson E., Variation in protein composition of wheat flour and its relationship to dough mixing behavior. Journal of Cereal Science 40 (2004) 31-39

[16] Yang, X. and C. E. Frazier (2016). Influence of organic fillers on rheological behavior in phenol-formaldehyde adhesives. International Journal of Adhesion and Adhesives 66: 93-98

[17] ASTM D854-14 Standard Test Methods for Specific Gravity of Soil Solids by Water Pycnometer, ASTM International, West Conshohocken, PA, 2014.

Chapter 6 Conclusions

6.1 Research summary

The impacts of organic fillers and extenders on the properties of phenol-formaldehyde resole (PF) resins that are formulated for veneer applications were investigated with different techniques.

The compositional analysis showed that walnut shell (*Juglans regia*), alder bark (*Alnus rubra*), almond shell (*Prunus dulcis*) exhibited chemical compositions that are typical for lignocellulosic materials. However, corn cob (furfural production) residue was distinctly different where it contains more than twice of extractives and little xylan due to the removal of furfural during the production.

The rheological analysis demonstrated the complex flow of these PF/filler formulations under shear forces and a similar flow behavior between whole wheat flour and starch/gluten blend used as extender, where transformation from mostly viscous to remarkably viscoelastic behavior was observed. Moreover, infrared study showed that alkali modification of wheat flour is accompanied by some changes in the physico-chemical structure of starch.

The basic rheological behavior of the formulations was subsequently used to develop an adhesive tack measurement based upon lubrication theory. In this work, the probe-tack test was adapted to a typical stress-controlled rheometer by using the normal force and displacement system to compress the adhesive between parallel plates. By employing a simple power law to describe the complex rheology of adhesives and a lubrication approximation for the viscous force, squeeze flow of adhesives between two flat, impermeable steels and between steel and porous wood can be successfully modeled. Compare to steel, lower magnitude of force on wood was observed, where the flow in the gap is coupled to the fluid flow in the porous substrate. However, deviations from theory were encountered as related to the method of adhesive application. Both meniscus force due to surface tension of adhesive pull around the edge of plate and viscous force due to the viscosity of adhesive operate inside the meniscus when adhesive was spread on the entire surface by a hard roller. Such is probably the case when wood veneer is cold-pressed (pre-pressed) in plywood manufacture where viscosity and surface tension effects were both involved.

6.2 Recommendations for future research

6.2.1 Rheological analysis

This work demonstrated the rheological complexity of the PF/filler formulations under shear forces. The complex rheological behavior within these formulations could arise from disintegration of filler particle aggregates on a non-colloidal scale, alkaline leachate from fillers and wheat flour within the liquid PF medium on a colloidal scale and/or polymeric adsorption of PF chains onto filler particle surfaces [1-5]. However, the precise nature and origin of this rheological complexity was unknown, and how these structures

could impact adhesive performance was not addressed, either. In addition, how these relate to the shear rates employed during industrial manufacture is another question. Future work should resolve these questions and relate to the manufacturing conditions.

6.2.2 Impact of wheat flour

The present work roughly demonstrated the effect of wheat starch and vital gluten used as extender on adhesive rheology and starch gelatinization within the formulation. Hydrated gluten is known to yield viscoelastic gluten complex [6,7]. Gelatinized starch in alkali exhibits non-Newtonian thixotropic or pseudoplastic in various conditions [8,9]. Petrofsky [10] demonstrated the existence of starch-gluten interactions. Future work should determine the effect of wheat starch, vital gluten, starch-gluten interaction and any filler-flour interaction within the formulation on adhesive properties, such as rheology, bond strength, and pre-press tack.

6.2.3 Adhesive tack

Both meniscus and viscous force operate inside the meniscus, which is probably the case when wood veneer is cold-pressed (pre-pressed) in plywood manufacture where viscosity and surface tension effects were both involved. Future work should quantify the contribution of viscous force and meniscus force to measured tack in various test conditions that are relative to plywood manufacturing. Improvements of pre-press tack in the manufacturing process should also be proposed.

6.3 Reference

[1] Yang, X. and C. E. Frazier (2016). Influence of organic fillers on rheological behavior in phenol-formaldehyde adhesives. International Journal of Adhesion and Adhesives 66: 93-98

[2] Potanin A., Thixotropy and rheopexy of aggregated dispersions with wetting polymer, J Rheol, 48 (2004) 1279-93.
[3] Johansson K., Larsson A., Ström G., Stenius P., Adsorption of phenol-formaldehyde resin onto cellulose, Colloids and Surfaces, 25 (1987) 341-56.

[4] Stack K., Dunn L., Roberts N., Adsorption studies of phenolformaldehyde resin onto cellulose fibres, Colloids and Surfaces A: Physicochemical and Engineering Aspects, 70 (1993) 23-31.

[5] Glasser W.G., Kaar W.E., Jain R.K., Sealey J.E., Isolation options for non-cellulosic heteropolysaccharides (HetPS), Cellulose, 7 (2000) 299-317.

[6] Uthayakumaran, S., Gras, P.W., Stoddard, F.L., Bekes, F., Effect of varying protein content and glutenin-to-gliadin ratio on the functional properties of wheat dough. Cereal Chemistry 76 (1999) 389–394.

[7] Alexander R.J., Krueger R.K., Plywood adhesives using amylaceous extenders comprising finely ground cereal-derived high fiber by-product, Washington, DC: U.S.

Patent and Trademark Office, 1978.

[8] Maher, G. G. : Alkali gelatinisation of flours. Starch/Starke 35 (1983), 271-276

[9] Ragheb A.A., Tawfik S., Cairo D., Gelatinization of starch in aqueous alkaline solutions. Starch/Starke 46 (1995), 338-345

[10] Petrofsky K.E., Hoseney R.C., Rheological properties of dough made with starch and gluten from several cereal sources. Cereal Chem. 72(1995): 53-58.